Stable isotopes (H, O, S) signatures evidencing evolutionary trends of Brazilian spas groundwaters

Albert Soler[1] and Daniel Marcos Bonotto[2*]

[1] Grup MAiMA, SGR Mineralogia Aplicada, Geoquímica i Geomicrobiologia, Departament de Mineralogia, Petrologia i Geologia Aplicada, Research Group of Mineralogía Aplicada y Medio Ambiente (MAiMA), Facultat de Ciències de la Terra, Universitat de Barcelona (UB), c/ Martí i Franquès s/n, 08028 Barcelona, Spain

[2]Instituto de Geociências e Ciências Exatas-IGCE, Universidade Estadual Paulista-UNESP, Av. 24-A No. 1515, P.O. Box 178, CEP 13506-900, Rio Claro, São Paulo, Brazil; e-mail: danielbonotto@yahoo.com.br

[*]Corresponding author

Abstract

This paper reports a stable isotope (H, O, S) study of groundwater samples (25) in 10 spas from southeast Brazil. They are cold (25°C, 36%), hypothermal (25-33°C, 60%) and mesothermal (33-36°C, 4%) waters; and are predominantly composed of bicarbonate, carbonate and sodium. Dissolved sulfate is the dominant anion in one water sample and its concentration increased with increase in pH, electrical conductivity (EC) and total dissolved solids (TDS) values in the samples. ^{2}H and ^{18}O data reported in the literature for circa 700 rainwater samples collected in São Paulo State and Brasília airport, Brazil, were used to construct the following regional meteoric waterline (RMWL): $\delta^{2}H$ V-SMOW (‰) = 8.06 $\delta^{18}O_{water}$ V-SMOW (‰) + 12.85. The H-O isotopes of the studied groundwater samples show a $\delta^{18}O_{water}$ variation of –14.1 to –5.3‰ V-SMOW, whereas the $\delta^{2}H$ range was –66.5 to –31.7‰ V-SMOW, which was plotted on or near the RMWL, suggesting a meteoric origin for them. However, one hypothermal water sample (29°C) plotted away from this RMWL, and is from a deep fractured aquifer which mainly occurs in fenitization aureole rocks surrounding the carbonatite complex at Araxá spa, Minas Gerais State, and a magmatic hydrothermal water may contribute to this water sample. The use of both $\delta^{34}S_{sulfate}$ and $\delta^{18}O_{sulfate}$ values in the selected sites permitted the plotting of a mixture line of the dissolved sulfate in the different aquifer systems of this study, considering two major sources as endmembers: sulfide oxidation, SOX ($\delta^{34}S_{sulfate}$= +1‰ and $\delta^{18}O_{sulfate}$= +1‰) and sulfates possessing $\delta^{34}S_{sulfate}$= +9‰ and $\delta^{18}O_{sulfate}$= +21‰ (OSW). This is an unusual isotopic composition opposite from that of sea water. The $\delta^{34}S_{sulfate}$ and $\delta^{18}O_{sulfate}$ values tend to increase with increase in dissolved sulfate concentration. The O-S isotopes signatures that deviated from the general mixture line could be due to several processes, including atmospheric deposition, SO_2 oxidation in the atmosphere, soil-derived sulfate, sulfide oxidation, evaporites dissolution and the presence of dissimilatory sulfate-reducing bacteria. Three sulfate isotope composition of spring waters from Águas da Prata spa in the Poços de Caldas alkaline massif (PCAM) represented endmember sources that defined a triangle around the remaining PCAM samples, as well as the samples from the crystalline basement, São Francisco craton, and Alto Paranaíba igneous province (APIP). Such triangle allows for estimation of the relative isotopic contribution in the different spas groundwaters, which is a new approach that focuses on the use of $\delta^{34}S_{sulfate}$-$\delta^{18}O_{sulfate}$ pair in environmental studies, and shows its usefulness in addition to other conventional hydrogeochemical fingerprints.

Keywords: spas groundwaters; southeast Brazil; H and O water isotopes; O and S isotopes in sulfates

1. Introduction

In Brazil, the use of thermal and mineral waters use is not a recent practice. It has been in existence since the arrival of European immigrants, mainly from Portugal. Thermal and mineral waters have been utilized in spas for baths and sometimes for bottling purposes. The commercialization of bottled waters in the country has been managed by DNPM (National Department of Mineral Production) who reported an amount higher than 1.5 billion liters at São Paulo State in 2007 (CPRM, 2012).

Some hydrogeochemical studies of Brazilian spas groundwaters have already been done under different approaches. For instance, several brands of bottled mineral waters were classified according to the activity concentration values of the natural radionuclides ^{226}Ra, ^{228}Ra and ^{210}Pb present in them (Godoy et al., 2001) or grouped according to the total dissolved solids (TDS) concentration (Bertolo et al., 2007), which also allow for the establishment of compositional relationships with host igneous, metamorphic and sedimentary silicate rocks of six aquifer systems of São Paulo State (Bulia and Enzweiler, 2018). Detailed hydrogeochemical surveys have been also conducted in some sites of the country like at Águas da Prata spa in São Paulo State, where major compounds, trace elements, the variations of the ^{2}H and ^{18}O compositions in rainwater and groundwater, and the natural radionuclides ^{222}Rn and ^{226}Ra were monitored for investigating their seasonal variation (Szikszay, 1981; Oliveira et al., 1998).

Additionally, the usefulness of the isotopic composition of water (H and O isotopes) has also been demonstrated in other studies conducted in Brazil, for instance, to establish the groundwater flow pattern in the northern portion of the Guarani Aquifer System (GAS) (Gastmans et al., 2010) and to propose a conceptual geochemical model of the GAS that suggests calcite dissolution driven by cation exchange in a relatively narrow front in São

Paulo State (Hirata et al., 2011). However, despite the knowledge obtained from such studies, the use of both $\delta^{34}S_{sulfate}$ and $\delta^{18}O_{sulfate}$ in hydrologic investigations in Brazil is incipient when compared to the country size due to the lack of measurements of the $^{34}S/^{32}S$ and $^{18}O/^{16}O$ ratios in dissolved SO_4^{2-}. If available, they do not consider the various lithologies present neither is there adoption of standardized procedures for sampling and analyzes. Thus, in Brazil, little approaches have been done focusing on the integrated use of the stable isotopes of H, O and S in the hydrological cycle, which are helpful to establish water origin and understand the processes that are related to water/rock interactions as their abundance in rainwater and groundwater allows for characterization of the host aquifers.

The $\delta^{34}S_{sulfate}$ and $\delta^{18}O_{sulfate}$ values have been used to determine SO_4^{2-} sources and pathways in the sulfur cycle, to better constrain the origin/fate of sulfate, to evaluate the transformations undergone by this solute, and to trace the groundwater flow in aquifers where the mineralogy may vary (Fritz and Fontes, 1980; Kroise and Van Everdingen, 1986; Krouse et al., 1991; Clark and Fritz, 1997; Tweed et al., 2006). Also, additional hydrologic applications worldwide include the tracing of anomalous TDS in surface waters of southern Alberta, Canada (Grasby et al., 1997), the indication of flow processes in aquifers of the Murray Basin, Australia (Dogramaci et al., 2001), the evaluation of the influence of mineral weathering on stream water sulfate in Vermont and New Hampshire, USA (Bailey et al., 2004), the acidification study in the Goose River watershed, Maine, USA (Sidle and Allen, 2004), the comparison of polluted and unpolluted sites in wetlands located in the British Isles and the Czech Republic, Central Europe (Novák et al., 2005), the degradation of groundwater quality in the Sichuan Basin, China (Li et al., 2006), the investigation of the mining-affected and undisturbed acidic drainage in the Animas River watershed, Colorado, USA (Nordstrom et al., 2007), the characterization of high arsenic groundwater in the Quaternary aquifers of Datong Basin, northern China (Xie et al., 2009), the determination of

111 the sources of dissolved organic sulfur in the Archer Creek Catchment, USA (Kang et al.,
112 2014), and to improve definitions of groundwater catchment zones in the Province of
113 Malaga, Spain (Jiménez-Madrid et al., 2017), among others.

114 This paper therefore reports a novel isotopic (H, O, S) dataset for spas groundwaters
115 from southern Brazil. The water isotopes H and O in rainwater and groundwater have been
116 used for identifying the water origin and mixing processes occurring due to water-rock/soil
117 interactions, whereas the $\delta^{34}S_{sulfate}$ and $\delta^{18}O_{sulfate}$ values have been used for evaluating
118 different sources of the dissolved sulfate in the related aquifer systems.

119

120 **2. Study area**

121

122 The groundwater samples (25) were taken from springs and pumped tubular wells from 10
123 spas located in the states of São Paulo (SP) and Minas Gerais (MG), Brazil: ASP-Águas de
124 São Pedro (2), ADP-Águas da Prata (4), ADL-Águas de Lindóia (1), TEI-Termas de Ibirá
125 (5), SLO-São Lourenço (2), CAM-Cambuquira (1), CAX-Caxambu (1), PDC-Poços de
126 Caldas (4), PRV-Pocinhos do Rio Verde (3) and AXA-Araxá (2). The water samples were
127 provided from different aquifer systems in the Paraná and Southeastern Shield
128 hydrogeological provinces at various geological contexts as reported by Mente (2008) (Fig. 1
129 and Table 1). The samples and spas codes are the same adopted by Bonotto (2016) in a
130 previous hydrogeochemical study.

131 The ASP and TEI spas are located in Paraná basin, a huge sedimentary area situated
132 between the parallels 10°-20° southern latitude and meridians 47°-64° western longitude,
133 comprising southern Brazil, Paraguay, Uruguay and Argentina. The basin constitutes a
134 geotectonic unit established over the South American Platform since the Lower Devonian or
135 Silurian (Almeida and Melo, 1981). The basal sandstones of Furnas Formation (Early

136 Devonian) are overlaid by the following units (Fig. 1): Itararé Subgroup (diamictites and
137 sandstones) and Tatuí Formation (siltstones and sandstones), both comprising the Tubarão
138 Aquifer System (Almeida and Melo, 1981); Passa Dois Group (fine shales, mudstones,
139 siltstones, and layers of dolomites), often considered an aquiclude due to the low
140 permeability lithotypes (Iritani and Ezaki, 2012); Pirambóia and Botucatu formations,
141 forming the Guarani Aquifer System (GAS), one of the largest aquifer units of the world
142 (Gilboa et al., 1976); Serra Geral Formation (basalt flows and dikes generated by the breakup
143 of Gondwana Supercontinent during Mesozoic Era) (Almeida and Melo, 1981), representing
144 the unique fractured aquifer unit in Paraná Basin; Bauru Group (sandstones, siltstones,
145 mudstones and locally conglomerates and limestones) (Fernandes, 2004), comprising the top
146 unit of the sedimentary sequence. In ASP spa, the groundwater from Tubarão Group was
147 pumped to the surface from wells exhibiting the following depths: GIO- 625 meters below ground
148 surface; JUV- 469 meters below ground surface (Kimmelmann et al., 1987). Other aquifers of
149 more restricted occurrence in the sedimentary domain (porous flow) at São Paulo State are
150 Taubaté, São Paulo and Cananéia (Iritani and Ezaki, 2012) (Fig. 1).

151 Several spas of this study are located in the Central South Fractured domain (Fig. 1 and
152 Table 1). The groundwater sample LIN (ADL spa) discharges through
153 fractures/fissures/faults in migmatites (Del Rey, 1989) which is a common rock type that
154 occurs at Águas de Lindóia area (Zanardo, 1987). The ADP, PDC and PRV spas are located
155 in Poços de Caldas alkaline massif (PCAM) that comprises a suite of alkaline volcanic and
156 plutonic rocks (mainly phonolites and nepheline syenites) whose evolutionary history started
157 with major early volcanism involving ankaratrites (biotite-bearing nephelinite), phonolite
158 lavas, and volcano-clastics (Schorscher and Shea, 1992). Extensive number of faults,
159 fractures and fissures exert an important control on the drainage system and hydrogeological
160 framework of the PCAM (Holmes et al., 1992). The groundwaters from PDC and PRV spas

161 discharge through crystalline fractured rocks (Cruz and Peixoto, 1989), whilst the following
162 springs were sampled at ADP spa (Szikszay, 1981): BOI (discharges into sandstones), VIT
163 (discharges through fissures in diabase), PLA and POL (discharge through volcanic tuffs,
164 phonolites and eudialite-bearing nepheline syenites).

165 The AXA spa is located at the Alto Paranaíba igneous province (APIP), including the
166 renowned Araxá carbonatite circular intrusion (diameter ~4.5 km) (Traversa et al., 2001).
167 The APIP comprises a diverse suite of ultrapotassic-potassic, ultramafic-mafic, silica-
168 undersaturated lavas and hypabyssal intrusions with very high concentrations of
169 incompatible trace elements and rare earths elements (REEs) (Gibson et al., 1995; Gomes
170 and Comin-Chiaramonti, 2005). Two springs were sampled at AXA spa: DBJ- associated to
171 a free to semi-confined granular aquifer system that occurs in the weathered mantle of the
172 carbonatite complex; AJU- related to a deep fractured unconfined to semi-confined aquifer,
173 mainly occurring in rocks surrounding the carbonatite complex (Beato et al., 2000).

174 The SLO, CAM and CAX spas are located in an area characterized by minor alkaline
175 occurrences representing multi-stage intrusions emplaced into Late-Proterozoic metamorphic
176 rocks (CPRM, 1999). The main rocks in the region are biotite gneisses, migmatized
177 granitoids, protomilonites, milonite gneisses, metabasites intercalations secondarily cut by
178 pegmatoids veins, schists, weathered quartzites and alluvial deposits. The gneissic rocks in
179 Caxambu hill are cut by mafic dykes and alkaline breccias that constitute important recharge
180 areas of the fractured aquifers (CPRM, 1999).

181

182 **3. Sampling and analytical methods**

183

184 Each groundwater sample was collected during the dry season (June-September) to avoid the
185 contribution of recent recharged rainwater. Limitation of the samples number was due to the

study area size and the costs involved in field trips and analyses. All water samples are sometimes used for drinking purposes, whilst some are commercialized by private companies under different brands.

The groundwater samples were collected from taps/pipes installed in each spring/well, stored in polyethylene bottles and transported to LABIDRO-Isotopes and Hydrochemistry Laboratory, Rio Claro city, for chemical analysis. Temperature, electrical conductivity (EC), pH, redox potential (Eh), and dissolved gases (O_2, CO_2 and H_2S) were measured *in situ* to avoid losses/modification during the process of transportation. A flow-through cell (similar to models developed by Eijkelkamp, Netherlands) was used to prevent contact with the atmosphere, whilst portable digital meters (Digimed, Hanna and Hach) were employed for such readings.

The samples were preserved at 4°C in darkness before the chemical analysis. Each one was divided into different aliquots and unfiltered + unpreserved or filtered through 0.45 µm Millipore membrane + preserved with different acids, depending on the requirements of the analyzes. Bonotto (2006, 2016) detailed the principal steps involved in the physicochemical, dissolved gases and major ions characterization of the water samples, as well the detection limit of each analytical technique adopted.

The groundwater sampling and storage for ^{2}H and ^{18}O measurements followed the general guidelines proposed elsewhere (Clark and Fritz, 1997; Mook, 2000). The $\delta^{18}O$ and $\delta^{2}H$ readings were conducted at Geosciences Institute, University of Brasília, Brasília (DF), Brazil, by wavelength Cavity Ring Down Spectroscopy (CRDS) technique through Picarro L2120-i. The CRDS uses a beam from a single-frequency laser diode entering a cavity defined by three high reflectivity mirrors to support a continuous travelling light wave (Picarro, 2010). The results were expressed in parts per mil (‰) relative to the $^{18}O/^{16}O$ and $^{2}H/^{1}H$ ratios of the Vienna Standard Mean Ocean Water (V-SMOW). Three IAEA

(International Atomic Energy Agency) named international standards were used for data correction: VSMOW2 (δ^2H= 0‰; δ^{18}O= 0‰), SLAP2 (δ^2H= -427.5‰; δ^{18}O= -55.5‰), and GISP (δ^2H= -189.5‰; δ^{18}O= -24.76‰). Analytical uncertainties (1σ) on the samples readings were 1‰ for δ^2H and 0.2‰ for δ^{18}O, whilst the following equations were used for the data generation:

$$\delta^{18}O_{water} = \{[(^{18}O/^{16}O)_{sample}/(^{18}O/^{16}O)_{V\text{-}SMOW}] - 1\} \times 1000 \quad (1)$$

$$\delta^{2}H = \{[(^{2}H/^{1}H)_{sample}/(^{2}H/^{1}H)_{V\text{-}SMOW}] - 1\} \times 1000 \quad (2)$$

The groundwater samples analysis for $\delta^{18}O_{sulfate}$ and $\delta^{34}S_{sulfate}$ was conducted at the "Centres Cientific i Tecnics" from the University of Barcelona (CCiTUB), Barcelona, Spain. Each aliquot was acidified with HCl and a barium chloride saturated solution was added in excess to variable sample volume for precipitating ~50 mg of $BaSO_4$. The precipitation was held at ~100°C in order to prevent $BaCO_3$ formation. The hot solution was allow to rest for 1-3 days for the precipitate formed to settle down; and the solution was filtered using a 3 µm paper filter, dried at room temperature (7-10 days), inserted into a Schott glass vial and heated for 3 h at 100°C prior to the isotopic analyses in order to remove humidity. $\delta^{34}S_{sulfate}$ was analyzed in a Carlo Erba Elemental Analyzer (EA) coupled in continuous flow to a Finnigan Mat Delta plus XP IRMS. $\delta^{18}O_{sulfate}$ was analyzed in duplicate with a ThermoQuest TC/EA unit (high temperature conversion elemental analyzer) with a Finnigan Mat Delta plus XP IRMS. The $\delta^{18}O_{sulfate}$ and $\delta^{34}S_{sulfate}$ data (in ‰) were determined by the equations:

$$\delta^{18}O_{sulfate} = \{[(^{18}O/^{16}O)_{sample}/(^{18}O/^{16}O)_{V\text{-}SMOW}] - 1\} \times 1000 \quad (3)$$

$$\delta^{34}S_{sulfate} = \{[(^{34}S/^{32}S)_{sample}/(^{34}S/^{32}S)_{V\text{-}CDT}] - 1\} \times 1000 \quad (4)$$

where $(^{34}S/^{32}S)_{V\text{-}CDT}$ is the Vienna scaled $^{34}S/^{32}S$ ratio from troilite (FeS) of the iron meteorite Cañyon Diablo and $(^{18}O/^{16}O)_{V\text{-}SMOW}$ is the $^{18}O/^{16}O$ ratio of the V-SMOW. According to Coplen (2011), for normalization of analyses, the following international and laboratory standards were employed: $\delta^{34}S_{sulfate}$ results- three international standards (NBS-

127, SO5, SO6) and one internal laboratory standard (CCIT-YCEM; $\delta^{34}S$= +12.8 ‰); $\delta^{18}O_{sulfate}$ results- three international standards (NBS-127, SO6, USGS-34) and two internal laboratory standards (CCIT-YCEM, $\delta^{18}O$= +17.6‰; CCIT-ACID, $\delta^{18}O$= +13.2‰). The reproducibility (1σ) of the samples as calculated from standards systematically interspersed in the analytical batches corresponded to ±0.2‰ for $\delta^{34}S_{sulfate}$ and ±0.5‰ for $\delta^{18}O_{sulfate}$.

4. Results

Table 2 shows the physicochemical and major hydrochemical data of the water samples focused on this study, including the parameter W that corresponds to the TDS removal rate. W (in ton/yr) was estimated by using the equation W=D×C, where C is the TDS concentration, and D is the water source discharge as reported by Del Rey (1989), Yoshinaga (1990) and Hurter et al. (1983), among others. The aquifers size and groundwater residence time are poorly known in most of the systems studied. Thus, other weathering rates or dissolution rates such as those parameters reported by Andrews and Wood (1972) could not be estimated with confidence and so were not taking into account. Contrarily, calculation of W is easy and direct, providing the whole amount of TDS removed over time in each spring/well. The average TDS concentration that came from atmospheric deposition collected in 10 monitoring stations installed at São Paulo State was 6.6 mg/L (Cresswell and Bonotto, 2008). It corresponds to 12% of the lowest TDS value found in the water sample BOI (54 mg/L, Table 2), only 0.2% of the highest TDS value was obtained in the water sample AJU (2898 mg/L, Table 2), and about 0.9% of the average TDS concentration was obtained from the water samples (760 mg/L). Therefore, the effect of the atmospheric deposition in the W value may be only slightly significant for TDS<100 mg/L (water samples BOI, LIN, and DBJ).

261 The guidelines of the Brazilian Code of Mineral Waters for temperature (DFPM,
262 1966) allow classification of spas groundwaters as cold (25°C, 9 water samples - 36%),
263 hypothermal (25-33°C, 15 water samples - 60%), and mesothermal (33-36°C, 1 water sample
264 - 4%). The waters analyzed are reducing as indicated by the Eh-pH diagram shown in Fig. 2.
265 Fluoride is a constituent of health concern, exceeding the WHO (2011) guideline
266 reference value of 1.5 mg/L in 14 water samples (56%). The French mineral water brands
267 Quézac, Vichy Célestins, and Vichy Saint-Yorre also exhibit F^- levels above 1.5 mg/L, but
268 they represent only 16% of all European waters described by Eupedia (2016). High-fluoride
269 groundwaters have also been recognized in several aquifers worldwide (Reddy et al., 2010;
270 Edmunds and Smedley, 2013). The F^-/Cl^- molar ratios above 1 in several water samples from
271 PCAM highlight that F^- is dominant relative to Cl^-.
272 The Piper (1944) diagram as plotted from the Aquachem 4.0 software (Waterloo
273 Hydrogeologic, 2003) shows that bicarbonate (range of 0-1390 mg/L), carbonate (range of 0-
274 2160 mg/L) and sodium (range of 1.9-1510 mg/L) are the dominant ions in the studied water
275 sources (Fig. 2). Additionally, in terms of dissolved anions, such diagram shows that sulfate
276 (range of 3-225 mg/L) predominates in the GIO sample (ASP spa), whilst chloride (range of
277 2.1-48 mg/L) dominates in the BOI sample (ADP spa) (Fig. 2).
278 Statistical tests applied to dataset reported in Table 2 indicated significant Pearson
279 correlation coefficient (r) of EC with the following parameters: TDS (r=0.93), Na^+ (r=0.92),
280 ALK (r=0.81), Cl^- (r=0.80), SO_4^{2-} (r=0.74), and W (r=0.70). The EC-TDS relationship is a
281 logical requirement widely reported elsewhere (e.g. Hem, 1985). The pH values increase
282 with increase in the sulfate concentration which also correlates with TDS and W (Fig. 3). In
283 a previous study, Bonotto (1993) reported enhanced $^{234}U/^{238}U$ activity ratio (AR) associated
284 to higher W values in water samples from ADP spa. Thus, W=0.8 ton/yr and AR=4.0 (water
285 sample BOI), whilst W= 200 ton/yr and AR=8.3 (water sample PLA). The higher W values

suggested a ^{234}U enhancement in solution associated with the weathering increase in the aquifers (Bonotto, 1993).

Table 3 reports all stable isotopes (H, O, S) data obtained in this study. The $\delta^{18}O_{water}$ range was –14.1 to –5.3‰ V-SMOW, whereas the $\delta^{2}H$ range was –66.5 to –31.7‰ V-SMOW. Table 3 shows the highest $\delta^{34}S_{sulfate}$ values of GIO and JUV water samples (ASP spa) relative to other spas groundwaters. The lowest $\delta^{18}O_{sulfate}$ value (+2.3‰) was found at BOI spring (ADP spa) that also exhibits the lowest EC (40 µS/cm) and TDS concentration (54 mg/L). The $\delta^{34}S_{sulfate}$ and $\delta^{18}O_{sulfate}$ data in the spas groundwaters are plotted in Fig. 3 against the dissolved sulfate concentration. Progressive higher $\delta^{34}S_{sulfate}$ values occurred accompanying the dissolved sulfate concentration (or W) increase (Fig. 3). The $\delta^{18}O_{sulfate}$ values also tended to fit a linear relationship with the SO_4 concentration (Fig. 3) as they increased according to the sulfate levels increase.

Theoretical relationships involving sulfate-oxygen exchange rates at environmental temperatures in the presence of atmospheric oxygen have been pointed out by Van Stempvoort and Krouse (1994). They allowed the construction of a $\delta^{18}O_{sulfate}$ *versus* $\delta^{18}O_{water}$ diagram (Fig. 4), in which the two major fields comprised an area dominated by primordial sulfate or SO_2 oxidation in the atmosphere and another area of sulfates derived from sulfide oxidation. The $\delta^{18}O_{sulfate}$ and $\delta^{18}O_{water}$ data reported in this paper (Table 3) are plotted in Fig. 4, which shows that the lower $\delta^{18}O_{sulfate}$ data of the water samples BOI, BZA and DBJ are in the field of sulfates derived by sulfide oxidation. For other groundwaters, the $\delta^{18}O_{sulfate}$ values indicate that SO_4 is likely derived from a mixture of sources including atmospheric deposition, soil-derived sulfate, sulfide oxidation and evaporite dissolution.

4. Discussion

4.1. ^{2}H and ^{18}O in rainwater and groundwaters

The ^{2}H and ^{18}O dataset in rainwater corresponded to about 700 samples obtained from monitoring stations installed at different sites: Águas da Prata (SP) (Szikszay, 1981); São Carlos (SP) and Ribeirão Preto (SP) (Silva, 1983); Rio Claro (SP), São Pedro (SP), Botucatu (SP), Águas de Santa Bárbara (SP), Assis (SP) and Presidente Prudente (SP) (Soler i Gil and Bonotto, 2015); Santa Maria da Serra (SP), Piracicaba (SP), Campinas (SP), Bragança Paulista (SP), São Paulo (SP) and Brasília (DF, airport) (IAEA, 2017). ^{2}H and ^{18}O in rainwater showed wide dispersion, with $\delta^{18}O_{water}$ range of –21.5 to +4.9‰ V-SMOW (mean= -4.88‰) and $\delta^{2}H$ range of –162.0 to +43.2‰ V-SMOW (mean= -26.5‰). They scattered around the regional meteoric waterline (RMWL) (Fig. 5):

$$\delta^{2}H \text{ V-SMOW } (‰) = 8.06\ \delta^{18}O_{water} \text{ V-SMOW } (‰) + 12.85 \quad (5)$$

The $\delta^{2}H$ and $\delta^{18}O_{water}$ in precipitation worldwide tends to fit the following global meteoric water line (GMWL) as defined by Craig (1961) from analytical data:

$$\delta^{2}H = 8\ \delta^{18}O_{water} + 10 \quad (6)$$

Rozanski et al. (1993) confirmed its validity, defining equation 7 from the compilation of average annual ^{18}O and ^{2}H values in precipitation monitored at stations throughout the IAEA global network.

$$\delta^{2}H = 8.13\ \delta^{18}O_{water} + 10.8 \quad (7)$$

Therefore, the RMWL and GMWL slopes are practically the same, implying that both straight lines are paralells (Fig. 5). However, the deuterium excess of the RMWL is slightly higher (about +2 to +3‰) than that of the GMWL (Fig. 5). In general, differences in

333 the deuterium excess have been attributed to the moisture source regions over the oceans,
334 from which the atmospheric moisture for subsequent precipitation events is derived.
335 Martinelli et al. (1996) found out that large rivers and lakes are likely contributors of
336 evaporated water to the atmosphere, returning water in vapor form from the land to the
337 atmosphere, via plant transpiration. Thus, evaporation produces an increase of deuterium
338 excess in Amazonian rain waters (Martinelli et al., 1996), and, in this sense, the observed
339 higher deuterium excess values can be produced by the contribution of the land waters
340 evaporation as a source of water vapor to the atmosphere.

341 The $\delta^{12}H$ and $\delta^{18}O_{water}$ data in the spas groundwaters (Table 3) are also plotted in Fig.
342 5. Except for the AJU water sample (AXA spa), all other values fit the RMWL, indicating
343 that the groundwater origin in the different aquifer systems investigated is directly related to
344 the meteoric water precipitation.

345 Certain physicochemical processes have been pointed out as responsible for causing
346 deviations from the meteoric water line (IAEA, 1983; Hackley, 1996): evaporation, high-
347 and low-temperature exchange reactions with rock minerals, hydration of silicates, CO_2-
348 exchange reactions, H_2S-exchange reactions, and methanogenesis. The AJU water sample
349 (AXA spa) is hypothermal (29°C), obtained from a deep fractured aquifer mainly occurring
350 in rocks surrounding the carbonatite complex that is characterized by a fenitization (*in situ*
351 metasomatism of country rock) aureole surrounding it, which possess a ring structure and
352 ~2.5 km-thickness (Traversa et al., 2001; Gomes and Comin-Chiaramonti, 2005).
353 Fenitization processes involve chemical changes affecting 100-160 anions (O, OH, F) in the
354 crystalline system (Appleyard and Woolley, 1979; Kresten, 1988). Variation diagrams have
355 been sometimes constructed on the basis of 100-160 oxygens, showing the increase in most
356 cations with decreasing silica (Kresten, 1988). Some quantitative estimates of mass transfer
357 during fenitization assume that oxygen is immobile, but other O-isotopes studies have

358 indicated oxygen transfer promoted by a highly mobile fluid containing enhanced H_2O and
359 CO_2 levels (Yund and Anderson, 1974). Water-CO_2 equilibrium at low temperatures (10-
360 60ºC) produces an isotopic fractionation with ^{18}O-enrichment in CO_2 and ^{18}O-depletion in
361 water, without any significant change in the δ^2H values (Brenninkmeijer et al., 1983). Also,
362 Karolyte et al. (2017) reported that oxygen isotope deviations without a change in hydrogen
363 isotopes can be interpreted as the result of oxygen isotope equilibrium exchange between
364 CO_2 and water, mineral dissolution and re-precipitation, or isotopic exchange with minerals.
365 The AJU hypothermal water is poor in CO_2 but very rich in CO_3^{2-} (Table 2) due to
366 interactions with carbonate minerals from two principal Araxá fenitized lithological groups
367 (carbonatites and mica-rich rocks) (Traversa et al., 2001). Such mineral dissolution processes
368 could justify the lowest $\delta^{18}O_{water}$ observed in this water sample (Fig. 5).

369 Lower δ^2H and $\delta^{18}O_{water}$ values have been sometimes pointed out as a consequence of
370 higher altitude or more continental recharge zones, whereas higher δ^2H and $\delta^{18}O_{water}$ values
371 due to Rayleigh fractionation during the cloud exhausting (Clark and Fritz, 1997). A
372 convincent evaluation of these aspects is not feasible in the study area because of the limited
373 data availability. Also, there is no enough information on the predominant directions of
374 moisture sources and pathways in the atmospheric circulation, as well as the latitude and
375 continental effects influencing the isotopic composition of precipitation/groundwater. No
376 correlation was found in the preliminary statistical tests among the acquired δ^2H and $\delta^{18}O_{water}$
377 data and the corresponding spas altitude (Fig. 6). For instance, the water samples GIO-JUV
378 (ASP spa) and JOR-ADB-CGO-SRC-SEI (TEI spa) are in equivalent altitudes (~450-470 m)
379 but their δ^2H and $\delta^{18}O_{water}$ values differ considerably: mean δ^2H = -33.6‰ (ASP spa) and
380 -64.4‰ (TEI spa); mean $\delta^{18}O_{water}$ = -5.5‰ (ASP spa) and -9.6‰ (TEI spa). This finding
381 probably could be explained by the location of the recharge zones for both spas at different
382 altitudes, i.e. higher for TEI spa and lower for ASP spa. Thus, for confirming this hypothesis,

383 further work is necessary in order to determine the recharge areas of the different aquifer
384 systems in the spas.
385
386 *4.2. Evolutionary trends from sulfur and oxygen isotopes in sulfates*
387
388 In general, dissolved sulfates that originated from evaporate dissolution are easy to identify
389 because of their characteristic isotopic composition of $\delta^{34}S_{sulfate}$>10‰ and $\delta^{18}O_{sulfate}$>12‰
390 (Claypool et al., 1980). Highly positive $\delta^{34}S_{sulfate}$ (>20‰) was found in groundwaters GIO
391 and JUV from ASP spa (Table 3). The Permian Irati Formation of the Passa Dois Group is
392 the main sedimentary sequence of the Paraná basin containing isolated ocurrences of marine
393 evaporites of Permo-Carboniferous age (Cabral Jr., 1991). Santos Neto (1993) identified
394 confined evaporitic conditions associated with mm- or cm-thick layers of gypsum and
395 nodular anhydrite close to ASP spa in a black shale-carbonate sequence of the Irati
396 Formation (SP). Unfortunatelly, Santos Neto (1993) did not record any $\delta^{34}S$ and $\delta^{18}O$
397 dissolved sulfate data in his study. However, Ferreira (2010) found $\delta^{34}S_{sulfate}$ values between
398 +4.9‰ and +7.4‰ in bituminous shales from Irati Formation at SIX (Superintendence of
399 Schist Industrialization) Quarry, Paraná State, and a value of +5.9‰ in a sulfur by-product
400 sample. These low $\delta^{34}S_{sulfate}$ values reflect SO_4 from sulfide oxidation in the shales as
401 reported elsewhere (Chao, 2011). Ferreira (2010) also reported highly positive $\delta^{34}S_{sulfate}$
402 values (+16.7‰ and +17.0‰) in gypsum samples from Santana Formation, Araripe basin,
403 northeastern Brazil, which correspond to sediments of marine facies deposited under
404 lacustrine evaporitic conditions. Such high $\delta^{34}S_{sulfate}$ values are compatible with those found
405 in dissolved SO_4 in groundwaters GIO and JUV (ASP spa).
406 Different evolutionary/mixing trends from the acquired $\delta^{34}S$ and $\delta^{18}O$ data of the
407 dissolved sulfate samples may be suggested. A mixing line can be constructed considering

two major sources as end members (Table 3 and Fig. 7): sulfide oxidation, SOX ($\delta^{34}S_{sulfate}$= +1‰ and $\delta^{18}O_{sulfate}$= +1‰) and sulfates possessing $\delta^{34}S_{sulfate}$= +9‰ and $\delta^{18}O_{sulfate}$= +21‰ (OSW) that is an unusual isotopic composition opposite from that of sea water ($\delta^{34}S_{sulfate}$ = +21‰; $\delta^{18}O_{sulfate}$= +9‰).

Highly positive $\delta^{18}O_{sulfate}$ values close to +21‰ have been reported in Precambrian evaporites (Sakai, 1972; Claypool et al., 1980) or acid rain (Jedrysek, 2000) that may reach SO_4 levels of up to 59 mg/L in some sites (Jedrysek, 2000). Temperature and pressure gradients favor the water-rock isotopic exchange in geothermal fields and sedimentary sequences at depths of a few thousand meters (Iacumin et al., 1991). $\delta^{18}O_{sulfate}$ shifts for SO_4 in groundwaters flowing through sedimentary sequences have been recorded in different situations (Boschetti, 2013): high-enthalpy hydrothermal systems (T>150°C); low-enthalpy (T<150°C) sulfate-water systems. Iacumin et al. (1991) pointed out that highly positive oxygen isotope values (up to +15.3‰) exhibited by flood basalts from the Paraná basin would be the result of secondary post-eruptive hydrothermal exchange processes between rock and ^{18}O-enriched water. The ^{18}O-enriched water can be formed by isotopic exchange between normal (meteoric) groundwater and either the thick sedimentary sequence underlying the volcanic sequence in the Paraná basin or the crystalline basement rocks (Iacumin et al., 1991).

Bonotto (2016) estimated a temperature of 83°C for the water sample ADB (TEI spa) from SiO_2 geothermometer. Its corresponding $\delta^{34}S$ and $\delta^{18}O$ dissolved sulfate values practically coincide with those of the end-member OSW. The average geothermal gradient of the Paraná basin is 28°C/km (Vitorello et al., 1978), implying a temperature of ~130°C at the deeper portions (~5 km). These conditions are typical of low-enthalpy systems sometimes characterized by exchange reactions affecting the $\delta^{18}O_{sulfate}$-values (Boschetti, 2013) that could explain this unknown end-member ($\delta^{34}S_{sulfate}$ = +9‰; $\delta^{18}O_{sulfate}$= +21‰).

The lower $\delta^{34}S_{sulfate}$ and $\delta^{18}O_{sulfate}$ values from BOI spring (ADP spa) (Fig. 7) are in agreement with dissolved SO_4 provided from sulfides oxidation in the aquifer. The evolutionary line in Fig. 7 suggests that all samples resulted from a mixing between sulfates from sulfides oxidation and sulfates with the OSW isotopic composition, perhaps derived from dissolution of Permian evaporites exhibiting $\delta^{34}S_{sulfate}$= +9‰ (Claypool et al., 1980). Deviation from the line of mixture can be explained by sulfate reduction processes that seems very clear for the ASP spa springs.

Dissimilatory sulfate-reducing bacteria such as *Desulfovibrio desulfuricans*, among others, are recognized to cause sulfur isotope fractionations based on the following reaction in which CH_2O represents generic organic matter (Seal, 2006):

$$2\ CH_2O + SO_4^{2-} \rightarrow H_2S + 2\ HCO_3^-$$

The reaction shows that organic carbon is oxidized, while sulfate is reduced. The H_2S can be lost to the water column, reoxidized, fixed as iron-sulfide minerals or other sulfide minerals, or fixed as organic-bound sulfur (Seal, 2006). The enhanced H_2S concentration of ~3 mg/L in groundwater JUV from ASP spa (Table 2) is compatible with this process. The sequence of organic-rich shales and carbonates of the Irati Formation close to ASP spa has been extensively studied due to its importance as a potential hydrocarbons source rock of the Paraná Basin, exhibiting the potential to generate liquid hydrocarbons (Lisboa, 2006). Therefore, these high reducing conditions are favorable for the dissimilatory sulfate-reducing bacteria to gain energy for their growth by catalyzing chemical reactions using the organic carbon. The fractionation of sulfur isotopes between sulfate and sulfide during bacterial sulfate reduction is a kinetically controlled process in which ^{34}S and $^{18}O_{sulfate}$ are enriched in the sulfate relative to the sulfide (Seal, 2006). The highly positive $\delta^{34}S_{sulfate}$ values found in groundwaters GIO and JUV from ASP spa (Table 3 and Fig. 7) could be explained by sulfate reduction processes.

Thus, the ASP spa waters agree with a sulfate origin from dissolution of Permian-Triassic sulfate that has suffered sulfate reduction processes. The following trends are also observed in Fig. 7 for the isotopic composition of dissolved sulfate in waters: ADL spa- agreement with an origin from dissolution of Permian-Triassic sulfates whilst the Lower Proterozoic geological materials indicate a large flow path; TEI spa- agreement with the OSW end-member sulfate source; SLO, CAM and CAX spas- seems to result from a mixture between sulfates from sulfide oxidation and sulfates from Triassic evaporates dissolution or with the OSW end-member sulfate source; ADP spa- results from a mixture between sulfide oxidation and the OSW end-member sulfate source, whereas the deviation of one sample from the mixing line according to a sulfate reduction trend can be interpreted also as a participation of Permian-Triassic sulfate.

4.3. Mixing models from sulfur and oxygen isotopes in sulfates

Mixing models for identifying possible sulfate sources in the waters may be constructed from $\delta^{34}S$ and $\delta^{18}O$ signatures of dissolved sulfate in two major geological contexts:

1) Paraná sedimentary basin (TEI spa). If the measurement uncertainty of the $\delta^{34}S_{sulfate}$ values is discarded, the following straight line can be traced (Fig. 8): $\delta^{18}O_{sulfate}$ = -6.98‰ × $\delta^{34}S_{sulfate}$ + 83.09‰. It suggests that the water samples JOR and ADB are end-members, whereas the isotopic composition of the remaining samples (CGO, SRC, and SEI; $\delta^{34}S_{sulfate}$ = +9.2‰ and $\delta^{18}O_{sulfate}$ = +17.6‰) result from their mixing. Thus, the groundwater ADB would contribute ~30% of the sulfate isotopic composition in the mixture. However, if the measurement uncertainty of the $\delta^{34}S_{sulfate}$ values is taken into account, only the signature of the sample JOR would be different from the remaining samples that could be grouped

482 together into a distinct type (Fig. 8), perhaps due to the slightly enhanced dissolved sulfate
483 concentration in the sample JOR (Table 2).

484 2) Crystalline basement (ADL spa), PCAM (ADP, PDC, and PRV spas), APIP (AXA
485 spa) and São Francisco craton (SLO, CAX, and CAM spas). The sulfate isotopic
486 composition of all studied samples could be interpreted as the result of three end-member
487 sources corresponding to BOI/BZA, PLA, and VIT that define a triangle around the rest of
488 samples, allowing the estimation of distinct sulfate isotopes contribution in the different spas
489 groundwaters (LIN, POL, NOV, MAC, SIN, PEB, RIV, SMA, SJO, SL1, SL9, MAR, DBJ,
490 and AJU) (Fig. 8). The triangle vertices comprise groundwaters that are related to different
491 flow systems through distinct rock types occurring at ADP spa and belonging to the PCAM
492 geological context such as sandstones (end-member BOI; porous flow), basalts and diabases
493 (end-member VIT; fissures/fractures flow) and volcanic tuffs, phonolites and eudialite-
494 bearing nepheline syenites (end-member PLA; fissures/fractures flow). Some water samples
495 plotted inside the triangle (POL, NOV, MAC, SIN, PEB, RIV, SMA and SJO) also occur at
496 the PCAM, whereas the remaining ones (LIN, SL1, SL9, MAR, DBJ, and AJU) were
497 provided from groundwater systems that occur at the crystalline basement in São Paulo State,
498 APIP and São Francisco craton. Their sulfate source contribution can be successfully
499 estimated from the mixing proportions of the $\delta^{34}S$ and $\delta^{18}O$ sulfate signatures of the three
500 end-members in the triangle vertices similarly to several calculations realized by Bonotto
501 (2017) from the dissolved uranium concentration and AR data in a larger number of spas
502 groundwater samples of southeastern Brazil.

503

504 **5. Conclusion**

505

Bicarbonate, carbonate and sodium are the dominant ions in the studied water samples. The water isotopes data indicate that all samples fit the Regional Meteoric Water Line (RMWL), which suggest that the groundwater origin in the different aquifer systems investigated is directly related to the meteoric water precipitation. The interactions of the AJU hypothermal water (AXA spa) with carbonate minerals from two principal Araxá fenitized lithological groups (carbonatites and mica-rich rocks) can justify its lowest $\delta^{18}O_{water}$ value pointing out of the RMWL. No statistical correlation between the $\delta^{2}H$ and $\delta^{18}O_{water}$ data and respective spas altitude can explain the water isotopic variation. Further work is necessary to determine the recharge area of the different aquifer systems in the spas in order to confirm this hypothesis. The $\delta^{34}S_{sulfate}$ values tend to be progressively higher according to the enhancement of the dissolved sulfate concentration and the increase in the TDS removal rate (W) as estimated after multiplying the water sample discharge by the TDS concentration. The dissolved sulfate isotopic composition of the spas groundwaters results from different contribution sulfates from diverse origins, i.e. sulfates from sulfide oxidation and sulfates from sulfate dissolution of two sources: a) Permian evaporites; b) unknown origin characterized by $\delta^{34}S_{sulfate}$= +9‰ and $\delta^{18}O_{sulfate}$= +21‰ (OSW) that is an unusual isotopic composition opposite from that of sea water. The OSW isotopic composition is very similar to that of the sample ADB and can be explained by exchange reactions affecting the $\delta^{18}O_{sulfate}$-values in low-enthalpy systems. Also, sulfate reduction processes seem to be very clear for the water samples of ASP spa, which makes it possible to explain deviation from the mixing line for these three sulfate sources. The sulfate isotope composition of all studied samples can be interpreted as the result of three sulfate endmember sources corresponding to BOI/BZA, PLA, and VIT. They define a triangle around the remaining samples, making it possible to estimate the diverse sulfate contribution in the different spas groundwaters LIN, POL, NOV, MAC, SIN, PEB, RIV, SMA, SJO, SL1, SL9, MAR, DBJ, and AJU.

Acknowledgments

FAPESP-Foundation Supporting Research in São Paulo State (Grant No. 2016/03054-2) and CNPq-National Council for Scientific and Technologic Development (Grant No. 301462/2011-9) in Brazil are greatly thanked for financial support of this investigation. This work has also been financed by the project CGL2014-57215-C4-1-R from the Spanish Government, and partially by the project 2014SGR-1456 from the Catalan Government. The *Centres Científico-Tècnics* of the *Universitat de Barcelona* is also acknowledged for the sulfate isotopic analysis. Dr. Luis H. Mancini from Geosciences Institute, University of Brasilia, Brasilia, Brazil, is greatly thanked for H and O isotopes analysis of the spas groundwaters.

References

Almeida, F.F.M., Melo, M.S., 1981. The Paraná basin and Mesozoic volcanism. In: IPT (Technological Research Institute of São Paulo State) (Ed.), Geological map of São Paulo State. Promocet, São Paulo, v. 1, pp. 46-81. Portuguese.

ANA (Brazilian National Agency of Waters), 2014. Outcrop map of Brazilian aquifers: groundwater availability from major aquifer systems. Brasilia (DF). Available from: <http://arquivos.ana.gov.br/institucional/sge/CEDOC/Catalogo/2014/MapaAreasDeAfloramentoDosAquiferos DoBrasil.pdf>. [cited 2017 Dec 10]. Portuguese.

Andrews, J.N., Wood, D.F., 1972. Mechanism of radon release in rock matrices and entry into groundwaters. Transactions of the Institute of Mineralogy and Metallurgy B81, 198-209.

Appleyard, E.C., Woolley, A.R., 1979. Fenitization: an example of the problems of characterizing mass transfer and volume changes. Chemical Geology 26, 1-15.

Bailey, S.W., Mayer, B., Mitchell, M.J., 2004. Evidence for influence of mineral weathering on stream water sulphate in Vermont and New Hampshire (USA). Hydrological Processes 18, 1639-1653.

Beato, D.A.C., Viana, H.S., Davis, E.G., 2000. Evaluation and hydrogeological diagnostic of aquifers from mineral waters at Barreiro do Araxá, MG, Brazil. In: ABAS (Brazilian Association of Groundwaters) (Ed.), Proc. I Joint World Congress on Groundwater. ABAS, Fortaleza, pp. 1-20. Portuguese.

563 Bertolo, R., Hirata, R., Fernandes, A., 2007. Hydrogeochemistry of mineral waters bottled in
564 Brazil. Revista Brasileira de Geociências 37, 2-15. Portuguese.
565 Bonotto, D.M., 1993. Enhancement of Uranium-234 in springwaters of Águas da Prata, São
566 Paulo, Brazil. Water Resources Research 29 (7), 2041-2048.
567 Bonotto, D.M., 2006. Hydro(radio)chemical relationships in the giant Guarani aquifer,
568 Brazil. Journal of Hydrology 323, 353-386.
569 Bonotto, D.M., 2016. Hydrogeochemical study of spas groundwaters from southeast Brazil.
570 Journal of Geochemical Exploration 169, 60-72.
571 Bonotto, D.M., 2017. The dissolved uranium concentration and $^{234}U/^{238}U$ activity ratio in
572 groundwaters from spas of southeastern Brazil. Journal of Environmental Radioactivity 166,
573 142-151.
574 Boschetti, T., 2013. Oxygen isotope equilibrium in sulfate–water systems: a revision of
575 geothermometric applications in low-enthalpy systems. Journal of Geochemical Exploration
576 124, 92-100.
577 Brenninkmeijer, C., Kraft, P., Mook, W.G., 1983. Oxygen isotope fractionation between CO_2
578 and H_2O. Chemical Geology 41, 181-190.
579 Bulia, I.L., Enzweiler, J., 2018. The hydrogeochemicstry of bottled mineral water in São
580 Paulo state, Brazil. Journal of Geochemical Exploration 188, 43-54.
581 Cabral Jr., M., 1991. Metallogenetic possibilities of the Paraná basin in São Paulo State:
582 phosphorites, evaporites and base metals. MS Dissertation, UNESP-São Paulo State
583 University, Rio Claro. Portuguese.
584 Chao Y-J.J., 2011. Major ion and stable isotope geochemistry of the Bow River, Alberta,
585 Canada. MS Dissertation, University of Calgary, Calgary, pp. 90-103.
586 Clark, I., Fritz, P., 1997. Environmental Isotopes in Hydrology. Lewis, Boca Raton (FL).
587 Claypool, G.E., Holser, W.T., Kaplan, I.R., Sakai, H., Zak, I., 1980. The age curves of sulfur
588 and oxygen isotopes in marine sulfate and their mutual interpretation. Chemical Geology 28,
589 199-261.
590 Coplen, T.B., 2011. Guidelines and recommended terms for expression of stable-isotope-
591 ratio and gas-ratio measurement results. Rapid Communication Mass Spectrometry 25 (17),
592 2538–2560.
593 CPRM (Brazilian Geological Survey), 1999. “Water Circuit from Minas Gerais State”
594 Project - Geoenvironmental studies of hydromineral springs from Águas de Contendas,

595 Cambuquira, Caxambu, Lambari and São Lourenço. CPRM, Belo Horizonte, pp. 1-142.
596 Portuguese.
597 CPRM (Brazilian Geological Survey), 2012. The Brazilian industry of mineral waters.
598 Available from: <http://www.cprm.gov.br/>. [cited 2017 Dec 4]. Portuguese.
599 Craig, H., 1961. Isotopic variations in meteoric waters. Science 133, 1702-1703.
600 Cresswell, R.G., Bonotto, D.M., 2008. Some possible evolutionary scenarios suggested by
601 Cl-36 measurements in Guarani aquifer groundwater. Applied Radiation and Isotopes 66,
602 1160-1174.
603 Cruz, W.B., Peixoto, C.A.M., 1989. Thermal waters of Poços de Caldas, MG: experimental
604 study of the water-rock interactions. Revista Brasileira de Geociências 19, 76-86.
605 Portuguese.
606 Del Rey, A.C., 1989. Hydrogeothermal study of the region of Águas de Lindóia, Amparo
607 and Socorro at northeast of São Paulo State. Ms Dissertation, USP- University of São Paulo,
608 São Paulo, 124 pp. Portuguese.
609 DFPM (Division for Supporting the Mineral Production), 1966. The mining code, the
610 mineral waters code and how applying research in a mineral deposit. 8th ed., Rep. 91. DFPM,
611 Rio de Janeiro. Portuguese.
612 Dogramaci, S.S., Herczeg, A.L., Schiff, S.L., Bone, Y., 2001. Controls on $\delta^{34}S$ and $\delta^{18}O$ of
613 dissolved sulfate in aquifers of the Murray Basin, Australia and their use as indicators of
614 flow processes. Applied Geochemistry 16, 475-488.
615 Edmunds, W.M., Smedley, P.L., 2013. Fluoride in natural waters. In: Selinus, O., Alloway,
616 B., Centeno, J.A., Finkelman, R.B., Fuge, R., Lindh, U., Smedley, P.L. (Eds.), Essentials of
617 Medical Geology. Springer, Heidelberg, pp. 311-336.
618 Eupedia, 2016. Mineral analysis of a few European mineral water brands. Available from:
619 <http://www. eupedia.com/europe/european_mineral_waters.shtml>. [cited 2017 Dec 2].
620 Fernandes, L.A., 2004. Lithostatigraphic map of the eastern portion of Bauru Basin (PR, SP
621 and MG), scale 1:10^6. Boletim Paranaense de Geociências 55, 53-66. Portuguese.
622 Ferreira, V.C.S.G.M., 2010. Geochemical characterization of samples of rocks and minerals
623 from sulfur isotopic ratios. MS Dissertation, COPPE/UFRJ – Federal University of Rio de
624 Janeiro, Rio de Janeiro, 61 pp. Portuguese.
625 Fritz, P., Fontes, J.C., 1980. Handbook of Environmental Isotope Geochemistry. Elsevier,
626 Amsterdam.

627 Gastmans, D., Chang, H.K., Hutcheon, I., 2010. Groundwater geochemical evolution in the
628 northern portion of the Guarani Aquifer System (Brazil) and its relationship to diagenetic
629 features. Applied Geochemistry 25, 16-33.
630 Gibson, S.A., Thompson, R.N., Dickin, A.P., Leonardos, O.H., 1995. High-Ti and low-Ti
631 mafic potassic magmas: Key to plume-lithosphere interactions and continental flood basalt
632 genesis. Earth and Planetary Science Letters 136, 149-165.
633 Gilboa, Y., Mero, F., Mariano, I.B., 1976. The Botucatu aquifer of South America, model of
634 an untapped continental aquifer. Journal of Hydrology 29, 65-179.
635 Godoy, J.M., Amaral, E.C.S., Godoy, M.L.D.P., 2001. Natural radionuclides in Brazilian
636 mineral water and consequent doses to the population. Journal of Environmental
637 Radioactivity 53, 175-182.
638 Gomes, C.B., Comin-Chiaramonti, P., 2005. Some notes on the Alto Paranaíba Igneous
639 Province. In: Comin-Chiaramonti, P., Gomes, C.B. (Eds.), Mesozoic to Cenozoic Alkaline
640 Magmatism in the Brazilian Platform. EDUSP, São Paulo, pp. 317-340. Portuguese.
641 Grasby, S.E., Hutcheon, I., Krouse, H.R., 1997. Application of the stable composition of SO_4
642 to tracing anomalous TDS in Nose Creek, southern Alberta, Canada. Applied Geochemistry
643 12, 567-575.
644 Hackley, K.C., Liu, C.L., Coleman, D.D., 1996. Environmental isotope characteristics of
645 landfill leachates and gases. Groundwater 34 (5), 827-836.
646 Hem, J.D., 1985. Study and interpretation of the chemical characteristics of natural waters.
647 U.S. Geological Survey, Water-Supply Paper 2254, 3rd ed.
648 Hirata, R., Gesicki A., Sracek, O., Bertolo, R., Giannini, P.C., Aravena, R., 2011. Relation
649 between sedimentary framework and hydrogeology in the Guarani Aquifer System in São
650 Paulo state, Brazil. Jouranl of South American Earth Sciences 31, 444-456.
651 Holmes, D.C., Pitty, A.E., Noy, D.J., 1992. Geomorphological and hydrogeological features
652 of the Poços de Caldas caldera analogue study sites. Journal of Geochemical Exploration 45,
653 215-247.
654 Hurter, S.J., Eston, S.M., Hamza, V.M., 1983. Brazilian collection of geothermal data –
655 Series 2: thermal springs. IPT (Technological Research Institute of São Paulo State), São
656 Paulo, pp. 1-111. Portuguese.
657 Iacumin, P., Piccirillo, E.M., Longinelli, A., 1991. Oxygen isotopic composition of Lower
658 Cretaceous tholeiites and Precambrian basement rocks from the Paraná basin (Brazil): the
659 role of water-rock interaction. Chemical Geology 86, 225-237.

660 IAEA (International Atomic Energy Agency), 1983. Isotope techniques in the
661 hydrogeological assessment of potential sites for the disposal of high-level radioactive
662 wastes. Tech. Rep. Series 228. IAEA, Vienna.
663 IAEA (International Atomic Energy Agency), 2017. Global Network of Isotopes in
664 Precipitation: the GNIP database. Vienna: IAEA (International Atomic Energy
665 Agency)/WMO (World Meteorological Organization). Available from:
666 http://www.iaea.org/water2017. [cited 2017 Dec 1].
667 Iritani, M.A., Ezaki, S., 2012. Groundwaters from São Paulo State. SMA-Environmental
668 Secretary São Paulo State, São Paulo, pp. 1-104. Portuguese.
669 Jedrysek, M.O., 2000. Oxygen and sulphur isotope dynamics in the SO_4^{2-} of an urban
670 precipitation. Water, Air & Soil Pollution 117, 15-25.
671 Jiménez-Madrid A, Castaño S, Vadillo I, Martinez, C., Carrasco, F., Soler, A., 2017.
672 Applications of hydro-chemical and isotopic tools to improve definitions of groundwater
673 catchment zones in a karstic aquifer: a case study. Water 9, 595. DOI:10.3390/w9080595.
674 Kang, P.G., Mitchell, M.J., Mayer, B., Campbell, J.L., 2014. Isotopic evidence for
675 determining the sources of dissolved organic sulfur in a forested catchment. Environmental
676 Science & Technology 48, 11259-11267.
677 Karolyte, R., Serno, S., Johnson, G., Gilfillan, S.M.V., 2017. The influence of oxygen
678 isotope exchange between CO_2 and H_2O in natural CO_2-rich spring waters: implications for
679 geothermometry. Applied Geochemistry 84, 173-186.
680 Kimmelmann, A.A., Yoshinaga, S., Murakami, H., Mattos, J.A., 1987. New
681 hydrogeological, hydrochemical and isotopic aspects of thermomineral waters from Águas
682 de São Pedro, São Paulo State. In: ABRH (Brazilian Association of Hydric Resources)
683 (Ed.), Proc. VII Brazilian Symposium of Hydrology and Hydric Resources, ABRH,
684 Salvador, pp. 26-41. Portuguese.
685 Krauskopf, K.B., Bird, D.K., 1995. Introduction to geochemistry. McGraw-Hill Inc., New
686 York (NY).
687 Kresten, P., 1988. The chemistry of fenitization: examples from Fen, Norway. Chemical
688 Geology 68, 329-349.
689 Krouse, H.R., Van Everdingen, R.O., 1986. Interpretation of oxygen isotope data for
690 sulphate in subsurface waters. In: IAGC (International Association of Geochemistry and
691 Cosmochemistry) (Ed.). Proceedings of the 5th International Symposium on Water-Rock
692 Interaction, 1986 Aug 8-17, Reykjavik. IAGC, Reykjavik, pp. 663-666.

693 Krouse, H.R., Gould, W.D., McCready, R.G.L., Raja, S., 1991. O incorporation into sulphate
694 during the bacterial oxidation of sulphide minerals and the potential for oxygen isotope
695 exchange between O_2, H_2O and oxidized sulphur intermediates. Earth and Planetary Science
696 Letters 107, 90-94.
697 Li, X.D., Masuda, H., Kusakabe, M., Yanagisawa, F., Zeng, H-A., 2006. Degradation of
698 groundwater quality due to anthropogenic sulfur and nitrogen contamination in the Sichuan
699 Basin, China. Geochemical Journal 40, 309-332.
700 Lisboa, A.C., 2006. Characterization of the organic geochemistry of Neo-Permian shales of
701 Irati Formation from the east border of Paraná basin, São Paulo State. MS Dissertation,
702 COPPE/UFRJ-Federal University of Rio de Janeiro, Rio de Janeiro. Portuguese.
703 Martinelli, L.A., Victoria, R.L., Sternberg, L.S.L., Ribeiro, A., Moreira, M.Z., 1996. Using
704 stable isotopes to determine sources of evaporated water to the atmosphere in the Amazon
705 basin. Journal of Hydrology 183, 191-204.
706 Mente, A., 2008. Hydrogeological map of Brazil. In: Feitosa, F.A.C., Manoel Filho, J.,
707 Feitosa, E.C., Demetrio, J.G. (Eds.), Hydrogeology – concepts and applic. CPRM-LABHID,
708 Rio de Janeiro, pp. 31-48. Portuguese.
709 Mook, W.G., 2000. Water sampling and laboratory treatment. In: UNESCO-IAEA (Eds.),
710 Environmental Isotopes in the Hydrological Cycle: Principles and Applications.v. 1,
711 UNESCO-IAEA, Paris-Vienna, pp. 167-178.
712 Nordstrom, D.K., Wright, W.G., Mast, M.A., Bove, D.J., Rye, R.O., 2007. Aqueous-sulfate
713 stable isotopes – a study of mining-affected and undisturbed acidic drainage. In: Church,
714 S.E., von Guerard, P., Finger, S.E. (Eds.), Integrated investigations of environmental effects
715 of historical mining in the Animas River watershed, San Juan County, Colorado. U.S.
716 Geological Survey, Denver, pp. 391-416.
717 Novák M, Vile MA, Bottrell SH, Štěpánová, M., Jačková, I., Buzek, F., Přechová, E.,
718 Newton, R.J., 2005. Isotope systematics of sulfate-oxygen and sulfate-sulfur in six
719 European peatlands. Biogeochemistry 76, 187-213.
720 Oliveira, J., Mazzilli, B.P., Sampa, M.H.O., Silva, B., 1998. Seasonal variations of Ra-226
721 and Rn-222 in mineral spring waters of Águas da Prata-Brazil. Applied Radiation and
722 Isotopes 49 (4), 423-427.
723 Picarro, 2010. Picarro L2120-i δD and $\delta^{18}O$ Analyzer. Picarro, Sunnyvale (CA).
724 Piper, A.M., 1944. A graphic procedure in the geochemical interpretation of water analyses.
725 Transactions of the American Geophysical Union 25, 914-928.

726 Reddy, D.V., Nagabhushanam, P., Sukhija, B.S., Reddy, A.G.S., Smedley, P., 2010. Fluoride
727 dynamics in the granitic aquifer of the Wailapally watershed, Nalgonda District, India.
728 Chemical Geology 269, 278-289.
729 Rozanski, K., Araguás-Araguás, L., Gonfiantini, R., 1993. Isotopic patterns in modern global
730 precipitation. In: Swart, P.K., Lohmann, K.C., McKenzie J., Savin, S. (Eds.), Climate
731 Change in Continental Isotopic Records. Geophys. Monogr. Ser. 78. AGU-American
732 Geophysical Union, Washington (DC), pp. 1-36.
733 Sakai, H., 1972. Oxygen isotopic ratios of some evaporites from Precambrian to recent ages.
734 Earth and Planetary Science Letters 15, 201-205.
735 Santos Neto, E.V., 1993. Geochemical characterization and depositional palaeoenvironment
736 of the Upper Carbonate-Pelitic Sequence from Assistência Member, Irati Formation in São
737 Paulo State, Paraná basin. MS Dissertation, UFRJ-Federal University of Rio de Janeiro, Rio
738 de Janeiro, 203 pp. Portuguese.
739 Schorscher, J.H.D., Shea, M.E., 1992. The regional geology of the Poços de Caldas alkaline
740 complex: mineralogy and geochemistry of selected nepheline syenites and phonolites.
741 Journal of Geochemical Exploration 45, 25-51.
742 Seal, R.R., 2006. Sulfur isotope geochemistry of sulfide minerals. Reviews in Mineralogy
743 and Geochemistry 61, 633-677.
744 Sidle, W.C., Allen, D., 2004. Importance of groundwater sulfate to acidification in the Goose
745 River watershed, Maine. Water Resources Research 40, W09402. DOI:10.1029/
746 2004WR003101.
747 Silva, R.B.G., 1983. Hydrochemical and isotopic study of groundwater from Botucatu
748 aquifer in São Paulo State. PhD Thesis, USP-University of São Paulo, São Paulo.
749 Portuguese.
750 Soler i Gil, A., Bonotto, D.M., 2015. Hydrochemical and stable isotopes (H, O, S) signatures
751 in deep groundwaters of Paraná basin, Brazil. Environmental Earth Sciences 73, 95-113.
752 Szikszay, M., 1981. Hydrogeochemistry of Águas da Prata springs, São Paulo State. Post
753 PhD Thesis, USP-University of São Paulo, São Paulo, 193 pp. Portuguese.
754 Traversa, G., Gomes, C.B., Brotzu, P., Buraglini, N., Morbidelli, L., Principato, M.S.,
755 Ronca, S., Ruberti, E., 2001. Petrography and mineral chemistry of carbonatites and mica-
756 rich rocks from the Araxá complex (Alto Paranaíba Province, Brazil). Anais da Academia
757 Brasileira de Ciências 73, 71-98.

758 Tweed, S.O., Weaver, T.R., Cartwright, I., Schaefer, B., 2006. Behavior of rare earth
759 elements in groundwater during flow and mixing in fractured rock aquifers: an example from
760 the Dandenong Ranges, southeast Australia. Chemical Geology 234,291–307.
761 Van Stempvoort, D.R., Krouse, H.R., 1994. Controls of $\delta^{18}O$ in sulfate. In: Alpers, C.N.,
762 Blowes, D.W. (Eds.), Environmental Geochemistry of Sulphide Oxidation. American
763 Chemical Society, Washington (DC), pp. 446-480.
764 Vitorello, I., Hamza, V.M., Pollack, H.N., Araújo, R.L.C., 1978. Geothermal investigations
765 in Brazil. Revista Brasileira de Geociências 8, 71-89. Portuguese.
766 Waterloo Hydrogeologic, 2003. AquaChem User´s Manual: Water Quality Data Analysis,
767 Plotting & Modeling. Waterloo Hydrogeologic, Waterloo, 276 pp.
768 WHO (World Health Organization). Guidelines for drinking-water quality. 4th ed. WHO
769 Press, Geneva.
770
771 Xie, X., Ellis, A., Wang, Y., Xie, Z., Duan, M., Su, C., 2009. Geochemistry of redox-
772 sensitive elements and sulfur isotopes in the high arsenic groundwater system of Datong
Basin, China. The Science of the Total Environment 407 (12), 3823-3835.
773 Yoshinaga, S., 1990. Hydrogeological, hydrogeochemical and isotopic studies of thermal
774 and mineral waters of Águas de Lindóia and Lindóia (SP). Ms Dissertation, USP-University
775 of São Paulo, São Paulo. Portuguese.
776 Yund, R.A., Anderson, T.F., 1974. Oxygen isotope exchange between potassium feldspar
777 and KCl solution. In: Hofmann, A.W., Giletti, B.J., Yoder Jr, H.S. Yund, R. A. (Eds.),
778 Geochemical transport and kinetics. Pub. 634. Carnegie Institution, Washington (DC), pp.
779 99-105.
780 Zanardo, A., 1987. Petrographic and micro-structural analysis of rocks from Águas de
781 Lindóia Sheet. Ms Dissertation, USP-University of São Paulo, São Paulo, 270 pp.
782 Portuguese.
783

Table 1. Description of the water samples analyzed in this paper.

Spa (State[1])	Latitude	Longitude	Altitude (m)	Spring (spr) or well (wl) identification	Hydrogeological Province[2]	Dominant flow	Major rock types	Geological context/age
ASP-Águas de São Pedro (SP)	23°35'30''S	47°53'38" W	470	Gioconda (wl)/GIO Juventude (wl)/JUV	Paraná	porous	sandstones	Botucatu Fm. (Jurassic) Pirambóia Fm. (Triassic) Itararé and Irati formations (Permian)
ADP-Águas da Prata (SP)	21°56'18''S	46°42'54" W	840	Platina (spr)/PLA Paiol (spr)/POL Vitória (spr)/VIT Boi (spr)/BOI	Paraná	fractures	diabases, phonolites, alkaline rocks silicified sandstones	Botucatu Fm. (Jurassic) Serra Geral Fm. (Jurassic-Cretaceous) Poços de Caldas intrusive complex (Cretaceous)
ADL-Águas de Lindóia(SP)	22°28'36''S	46°38'00" W	945	Lindália (spr)/LIN	Paraná	fractures	granites, gneisses, migmatites, schists, quartzites, limestones, dolomites	Amparo Gp. (Lower Proterozoic)
TEI-Termas de Ibirá (SP)	21°04'50''S	49°14'25" W	455	Jorrante (spr)/JOR Ademar de Barros (spr)/ADB Carlos Gomes (spr)/CGO Saracura (spr)/SRC Seixas (spr)/SEI	Paraná	porous and fractures	sandstones basalts	Bauru Gp. (Cretaceous) Serra Geral Fm. (Jurassic-Cretaceous)
SLO-São Lourenço (MG)	22°06'59''S	45°03'16" W	875	No. 1-Oriente (spr)/SL1 No. 9-Carbogasosa (spr)/ SL9	Southeastern shield	porous and fractures	ortogneisses, granulites migmatites, metassedimentary/ metavulcanossedimentary seq.	Paraíba do Sul, Barbacena, São João d´el Rei and Andrelândia Groups (Proterozoic), magmatic plutonic series (Brasiliano)
CAM-Cambuquira (MG)	21°52'13''S	45°19'03" W	950	Marimbeiro (spr)/MAR				
CAX-Caxambu (MG)	21°58'10''S	44°55'30" W	895	Beleza (spr)/BZA				
PDC-Poços de Caldas (MG)	21°47'18''S	46°33'45" W	1196	XV de Novembro (spr)/ NOV Macacos (spr)/MAC Sinhazinha (spr)/SIN	Southeastern shield	Fractures	alkaline rocks, phonolites, nepheline syenites, pyroclastics, volcanic tuffs	Poços de Caldas intrusive complex (Cretaceous)
PRV-Pocinhos do Rio Verde (MG)	21°55'20''S	46°23'20" W	1055	Pedro Botelho (spr)/PEB Rio Verde (spr)/RIV Samaritana (spr)/SMA São José (spr)/SJO				
AXA-Araxá (MG)	19º35'33"S	46º56'26"W	973	Dona Beja (spr)/DBJ Andrade Júnior (spr)/AJU	Southeastern shield	porous and Fractures	quartzites, schists, alkaline-carbonatitic rocks	Cretaceous, PreCambrian

[1]SP = São Paulo State, MG = Minas Gerais State; [2]According to Mente (2008).

Table 2. Physicochemical and major hydrochemical data of the water sources focused in this study.

Sample code	D ($\times 10^{-6}$ m^3/s)	Temp. (°C)	pH	Eh (mV)	EC (µS/cm)	DO (mg/L)	CO_2 (mg/L)	H_2S (µg/L)	ALK (mg/L)	SiO_2 (mg/L)	Fe_{tot} (mg/L)	Fe^{2+} (mg/L)	TDS (mg/L)	W (ton/yr)
GIO	4051	27.4	8.4	-59	3790	5.1	100	6	204	12.8	0.01	b.d.	1700	217.2
JUV	3472	26.7	8.6	-59	4730	2.8	88	3064	338	24.5	0.7	b.d.	1960	214.6
PLA	236	25.4	8.2	-5	1530	1.3	400	5	472	33.1	0.01	b.d.	936	7.0
POL	1756	25.8	8.2	-37	3630	3.1	800	12	1390	29.0	0.02	b.d.	2625	145.4
VIT	22	24.5	9.2	-150	3370	1.3	1032	2	1388	32.8	0.06	b.d.	1042	0.7
BOI	33	24.2	7.6	-154	40	3.8	128	4	17	18.6	0.2	0.01	54	0.06
LIN	3889	24.6	7.0	-3	360	5.7	136	4	76	37.5	0.02	0.02	86	10.6
JOR	n.a.	26.8	9.0	-144	660	2.0	0	13	99	34.3	0.01	b.d.	410	n.c.
ADB	n.a.	28.4	9.0	-145	670	2.6	0	3	130	32.4	0.01	b.d.	420	n.c.
CGO	1389	28.4	9.1	-147	680	1.3	0	5	98	34.6	0.05	b.d.	380	16.6
SRC	n.a.	28.7	9.2	-150	700	1.0	0	35	90	33.4	b.d.	b.d.	460	n.c.
SEI	n.a.	26.4	9.0	-138	640	2.4	0	8	105	37.3	b.d.	b.d.	455	n.c.
SL1	2778	25.6	6.0	-44	670	1.3	1420	b.d.	163	17.9	0.03	0.01	296	25.9
SL9	419	23.9	5.9	-57	640	1.0	1480	b.d.	162	21.3	3.7	0.04	295	3.9
MAR	102	25.5	5.8	-42	570	3.3	1200	4	130	60.9	2.3	0.02	249	0.8
BZA	21	23.9	6.4	-65	3010	1.8	1440	1	680	60.2	3.2	2.9	757	0.5
NOV	118	25.7	9.4	-53	920	1.4	0	259	196	28.4	0.04	b.d.	398	1.5
MAC	n.a.	32.1	9.6	-51	1450	0.8	0	1184	233	31.0	0.01	b.d.	579	n.c.
SIN	6	25.7	9.5	-90	1420	2.9	140	3	261	32.2	0.02	b.d.	574	0.1
PEB	694	35.7	9.6	-70	1400	1.2	0	383	252	28.5	0.06	b.d.	600	13.1
RIV	67	23.3	9.1	-133	1290	1.3	180	756	270	30.5	0.02	b.d.	567	1.2
SMA	67	23.9	9.0	-133	1300	1.4	80	522	291	28.3	b.d.	b.d.	773	1.6
SJO	75	22.0	9.0	-133	1290	1.3	60	528	318	29.3	b.d.	b.d.	424	1.0
DBJ	12537	22.1	7.5	-146	330	5.0	252	1	112	23.4	0.06	b.d.	70	27.7
AJU	1111	29.0	9.6	-141	6390	1.6	0	1980	2212	20.3	0.04	b.d.	2898	101.5

Sample code	Na^+ (mg/L)	K^+ (mg/L)	Ca^{2+} (mg/L)	Mg^{2+} (mg/L)	HCO_3^- (mg/L)	CO_3^{2-} (mg/L)	OH^- (mg/L)	Cl^- (mg/L)	F^- (mg/L)	NO_3^- (mg/L)	SO_4^{2-} (mg/L)	PO_4^{3-} (mg/L)
GIO	459.0	1.9	0.1	0.8	204	0	0	27.0	7.1	0.9	225	0.06
JUV	598.0	1.2	1.1	0.08	338	0	0	28.4	8.3	11.2	126	0.08
PLA	200.0	4.0	0.04	0.98	472	0	0	10.2	19.7	8.5	37	0.2
POL	532.0	9.8	0.02	1.0	1390	0	0	16.9	32.4	1.2	90	0.2
VIT	567.0	13.1	0.9	0.9	1134	254	0	23.5	18.4	6.6	111	0.09
BOI	1.9	8.3	0.06	0.7	17	0	0	24.5	0.3	1.3	11	0.05
LIN	15.7	4.0	0.02	0.6	76	0	0	9.3	0.4	8.7	11	0.5
JOR	87.8	0.4	2.3	b.d.	0	82	17	7.8	0.4	1.5	78	0.1
ADB	87.4	0.4	2.5	0.01	0	106	24	7.0	0.4	2.6	52	0.2
CGO	91.4	0.4	2.7	0.01	0	52	46	7.9	0.4	1.7	67	0.3
SRC	91.8	0.3	2.5	0.01	0	22	68	7.7	0.5	1.2	74	0.2
SEI	83.5	0.3	2.4	0.01	0	58	47	7.0	0.5	2.9	63	0.06
SL1	33.7	17.2	3.4	0.2	163	0	0	12.8	0.2	1.1	3	0.09
SL9	35.2	17.5	3.5	0.4	162	0	0	8.0	0.9	b.d.	3	0.07
MAR	14.9	13.0	3.3	0.5	130	0	0	2.5	0.5	0.8	4	0.2
BZA	108.8	25.2	5.0	0.4	680	0	0	5.6	2.3	18.1	4	0.1
NOV	112.9	6.9	0.6	0.02	70	126	0	4.6	13.6	11.1	41	0.08
MAC	183.0	10.4	0.5	0.03	0	150	83	6.0	22.2	3.3	76	0.1
SIN	180.0	9.6	0.7	0.03	31	230	0	5.8	23.0	1.0	73	0.09
PEB	183.0	11.1	0.7	0.04	4	248	0	5.7	22.2	1.9	75	0.1
RIV	182.0	9.3	2.1	0.01	86	184	0	7.9	25.2	1.0	76	0.2
SMA	182.7	10.5	2.3	0.02	123	168	0	7.5	26.4	1.0	78	0.05
SJO	178.0	10.6	2.4	0.02	142	176	0	7.3	26.0	1.3	78	0.07
DBJ	2.1	8.8	0.2	0.3	112	0	0	2.1	0.3	5.3	3	0.3
AJU	1510.0	14.9	0.4	0.1	52	2160	0	48.0	9.0	2.3	189	1.4

D = discharge; EC = Electrical Conductivity; DO = Dissolved Oxygen; ALK = Total Alkalinity; TDS = Total Dissolved Solids; W=D×C (D=discharge; C=TDS concentration); n.a.= not available; b.d. = below detection limit; n.c.= not calculated.

Table 3. Stable isotopes (H, O, S) data of the spas groundwaters analyzed in this study.

Sample code	$\delta^{2}H$ V-SMOW (‰)	$\delta^{18}O_{water}$ V-SMOW (‰)	$\delta^{34}S_{sulfate}$ V-CDT(‰)	$\delta^{18}O_{sulfate}$ V-SMOW (‰)
GIO	-35.5	-5.7	+23.6	+16.9
JUV	-31.7	-5.3	+26.9	+12.6
PLA	-57.1	-8.9	+8.0	+18.8
POL	-58.0	-8.9	+7.9	+14.5
VIT	-46.4	-7.3	+12.1	+9.1
BOI	-48.0[3]	-7.7[3]	+3.0	+2.3
LIN	-47.7[4]	-7.7[4]	+9.6	+11.8
JOR	-64.9	-9.7	+9.6	+16.3
ADB	-63.4	-9.4	+9.1	+20.6
CGO	-63.9	-9.5	+9.2	+17.6
SRC	-64.9	-9.6	+9.2	+16.7
SEI	-64.9	-9.7	+9.2	+18.4
SL1	-55.9	-8.9	+3.6	+6.9
SL9	-49.7	-7.6	+8.7	+8.4
MAR	-51.9	-8.0	+7.3	+6.2
BZA	-66.5	-10.3	+2.5	+2.6
NOV	-58.2	-9.0	+6.6	+7.2
MAC	-63.8	-9.7	+7.3	+6.0
SIN	-53.7	-7.8	+8.3	+6.7
PEB	-65.2	-10.1	+7.5	+12.6
RIV	-63.2	-9.7	+7.9	+13.9
SMA	-63.1	-9.9	+7.5	+13.3
SJO	-62.7	-9.8	+8.5	+12.0
DBJ	-48.8	-7.5	+5.0	+3.4
AJU	-64.0	-14.1	+5.0	+8.1
SOX[1]			+1.0	+1.0
OSW[2]			+9.0	+21.0

[1]SOX = Sulfide Oxidation (Van Stempvoort and Krouse, 1994);
[2]OSW = Opposite of the Sea Water (Fritz and Fontes, 1980; Krouse and Van Everdingen, 1986; Van Stempvoort and Krouse, 1994);
[3]Mean of the values reported by Szikszay (1981);
[4]Reported by Yoshinaga (1990).

FIGURE CAPTIONS

Figure 1. Spatial distribution in Brazil of the spas where groundwater samples were collected and its relation with outcropping aquifer systems. Spas codes: 1-ASP (Águas de São Pedro); 2-ADP (Águas da Prata); 3-PDC (Poços de Caldas); 4-PRV (Pocinhos do Rio Verde); 5-ADL (Águas de Lindóia); 6-SLO (São Lourenço); 7-CAX (Caxambu); 8-CAM (Cambuquira); 9-AXA (Araxá); 10-TEI (Termas de Ibirá). Base map modified from ANA (2014).

Figure 2. Data of the spas groundwaters of this study plotted (top) in an Eh-pH diagram as reported by Krauskopf and Bird (1995), and (bottom) in a Piper (1944) diagram including the presence of the anion fluoride.

Figure 3. The relationships among the pH, TDS, dissolved sulfate concentration, TDS removal rate (W), $\delta^{34}S_{sulfate}$ and $\delta^{18}O_{sulfate}$ data (Tables 2 and 3) of the spas groundwaters.

Figure 4. The $\delta^{18}O_{sulfate}$ and $\delta^{18}O_{water}$ data (Table 3) in the spas groundwaters plotted in the simplified diagram proposed by Van Stempvoort and Krouse (1994). The field A corresponds to the experimental area of sulfates derived by sulfide oxidation. Its upper boundary represents 63% of oxygen incorporation into SO_4 from H_2O, whereas the lower boundary represents the maximum 100% contribution of oxygen in SO_4 from H_2O, assuming no isotopic fractionation during oxygen incorporation from H_2O into SO_4 (Van Stempvoort and Krouse, 1994).

Figure 5. (Top) The regional meteoric waterline (RMWL: δ^2H V-SMOW (‰) = 8.06 $\delta^{18}O_{water}$ V-SMOW (‰) + 12.85) plotted from δ^2H and $\delta^{18}O_{water}$ values in circa 700 rainwater samples collected in São Paulo State and Brasília airport, Brazil. Data source: Szikszay (1981), Silva (1983), Soler i Gil and Bonotto (2015), IAEA (2017). (Bottom) The δ^2H and $\delta^{18}O_{water}$ data for the spas groundwaters (Table 3) plotted together with the global meteoric water line (GMWL) and regional meteoric waterline (RMWL).

Figure 6. Plots of the δ^2H *versus* $\delta^{18}O_{water}$ data against the spas altitude. The Pearson correlation coefficient is r=0.16 and r=0.22 for the δ^2H and $\delta^{18}O_{water}$ values, respectively.

Figure 7. Possible evolutionary/mixing trends evidenced by the $\delta^{18}O_{sulfate}$ and $\delta^{34}S_{sulfate}$ data (Table 3) of the spas groundwaters.

Figure 8. Plots of the $\delta^{18}O$ and $\delta^{34}S$ dissolved sulfate data (Table 3) of the spas groundwaters in mixing models for identifying possible sulfate sources.

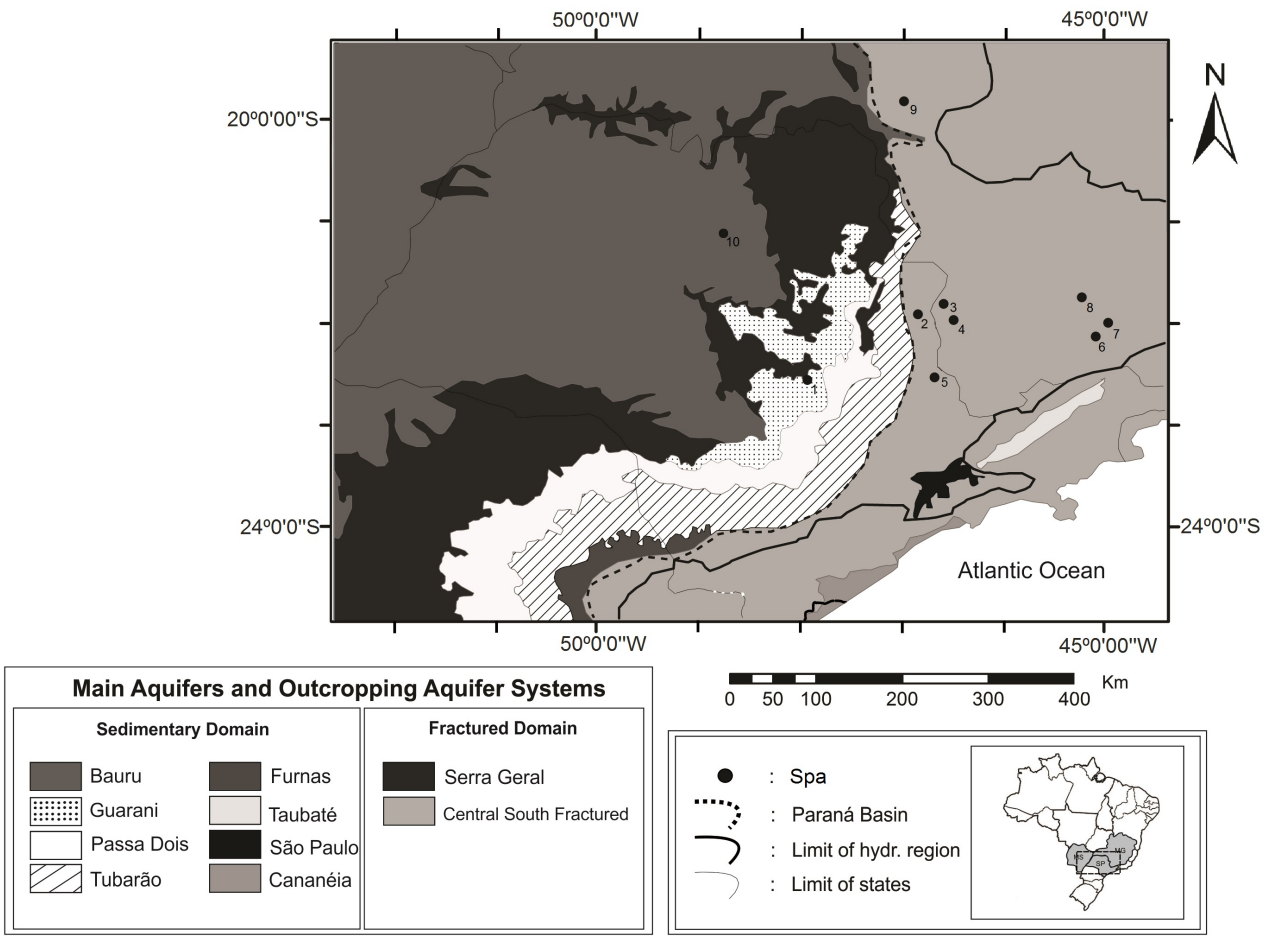
50º0'0"W
45º0'0"W
20º0'00"S
24º0'0"S
N
Atlantic Ocean
9
10
2
3
4
5
6
7
8
Main Aquifers and Outcropping Aquifer Systems
Sedimentary Domain
Bauru
Guarani
Passa Dois
Tubarão
Furnas
Taubaté
São Paulo
Cananéia
Fractured Domain
Serra Geral
Central South Fractured
0 50 100 200 300 400
Km
: Spa
: Paraná Basin
: Limit of hydr. region
: Limit of states

FIG. 1

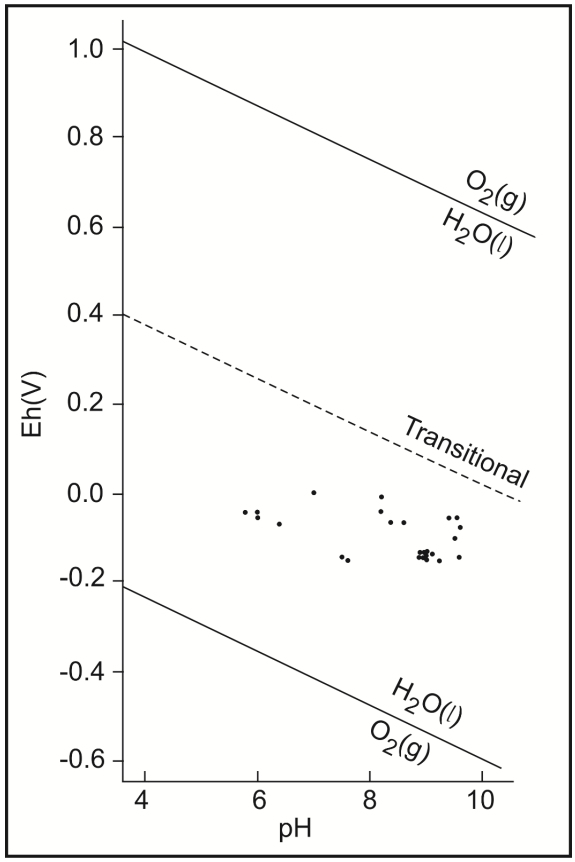
1.0
0.8
0.6
0.4
0.2
0.0
-0.2
-0.4
-0.6
Eh(V)
4
6
8
10
pH
O2(g)
H2O(l)
Transitional
H2O(l)
O2(g)

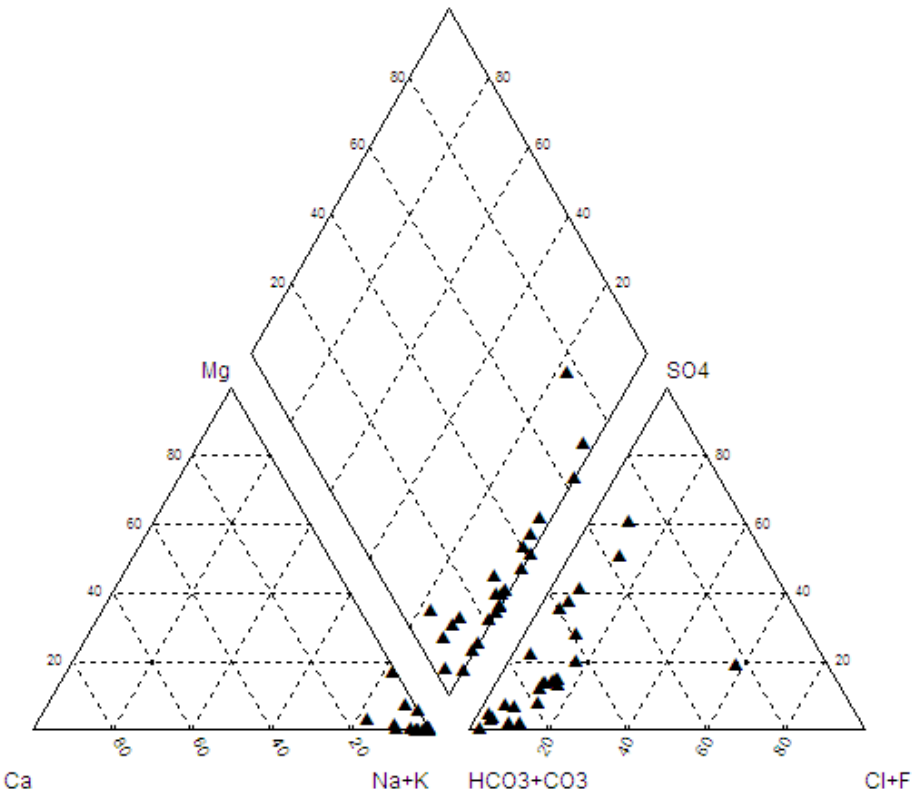
Mg
SO4
Ca
Na+K
HCO3+CO3
Cl+F

FIG. 2

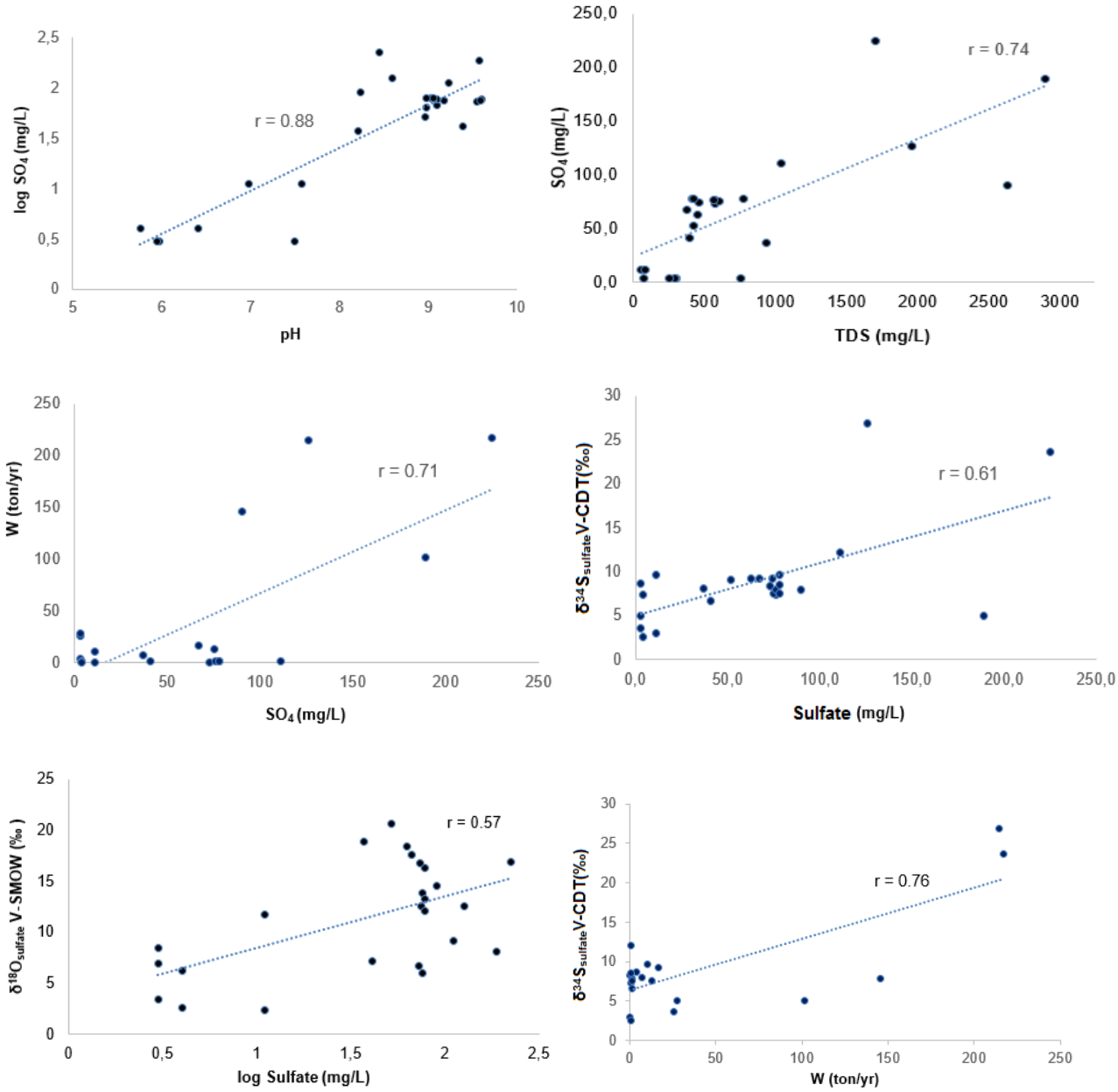
r = 0.88
log SO4 (mg/L)
pH
r = 0.74
SO4 (mg/L)
TDS (mg/L)
r = 0.71
W (ton/yr)
SO4 (mg/L)
r = 0.61
δ34Ssulfate V-CDT(‰)
Sulfate (mg/L)
r = 0.57
δ18Osulfate V-SMOW (‰)
log Sulfate (mg/L)
r = 0.76
δ34Ssulfate V-CDT(‰)
W (ton/yr)

FIG. 3

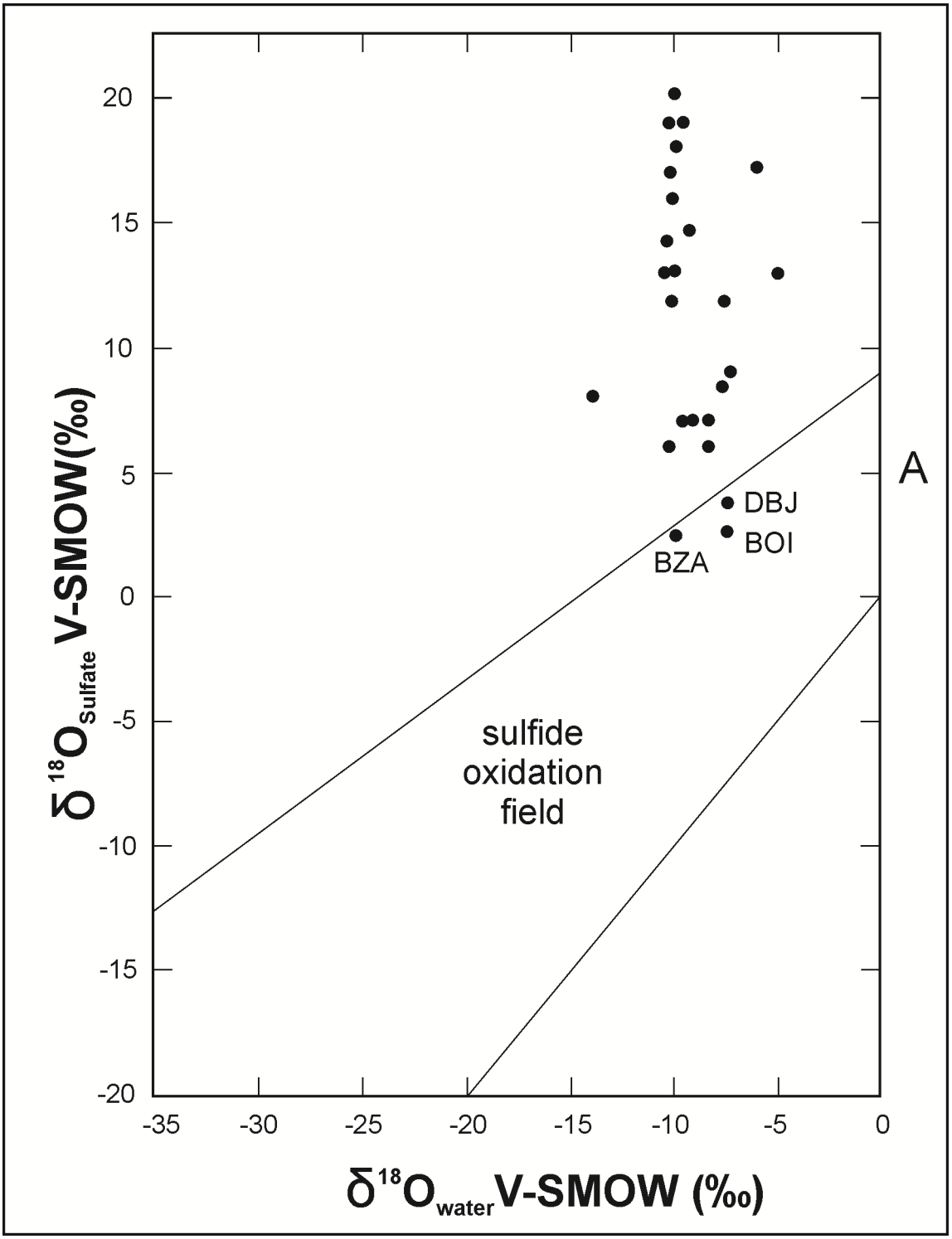
20
15
10
5
0
-5
-10
-15
-20
-35
-30
-25
-20
-15
-10
-5
0
δ18OSulfate V-SMOW(‰)
δ18Owater V-SMOW (‰)
A
DBJ
BOI
BZA
sulfide
oxidation
field

FIG. 4

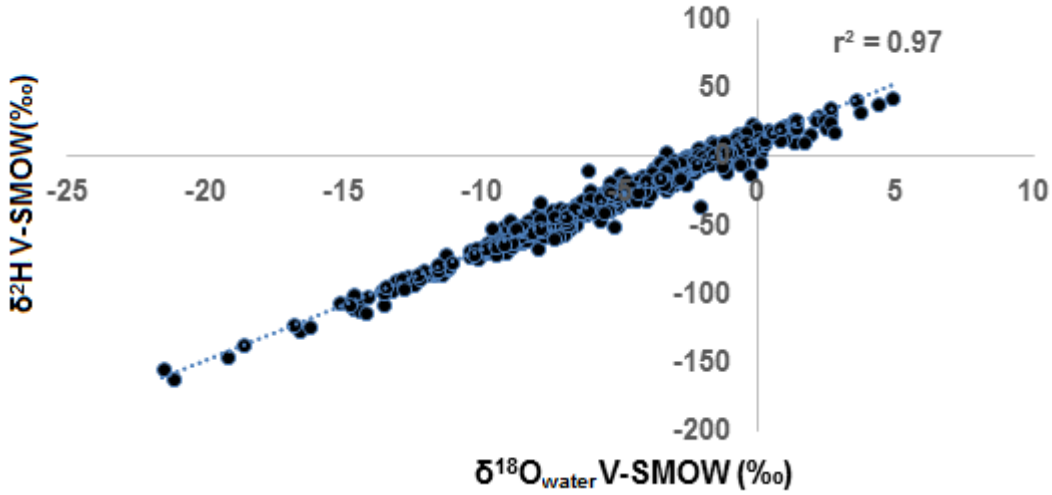
100
50
-50
-100
-150
-200
-25
-20
-15
-10
0
5
10
r² = 0.97
δ²H V-SMOW(‰)
δ¹⁸O water V-SMOW (‰)

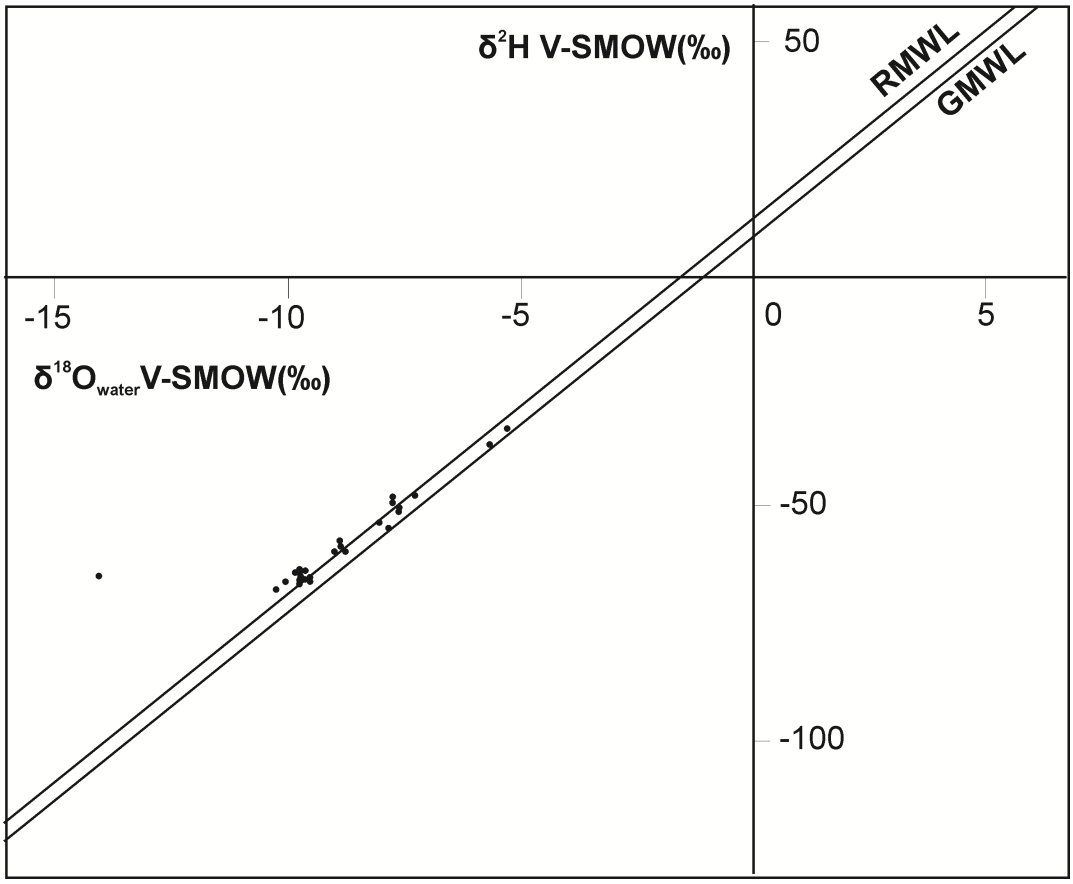
δ²H V-SMOW(‰)
50
RMWL
GMWL
-15
-10
-5
0
5
δ¹⁸O water V-SMOW(‰)
-50
-100

FIG. 5

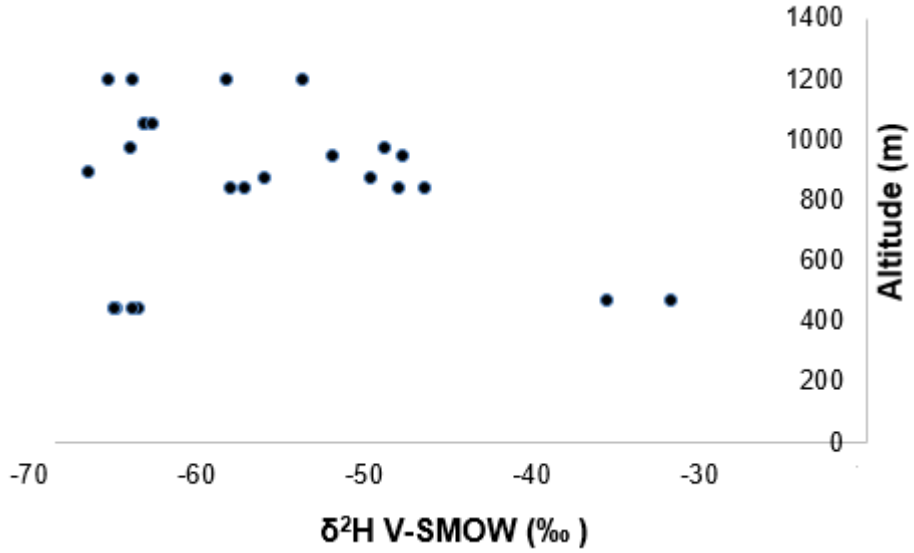
1400
1200
1000
800
600
400
200
0
Altitude (m)
-70
-60
-50
-40
-30
δ²H V-SMOW (‰)

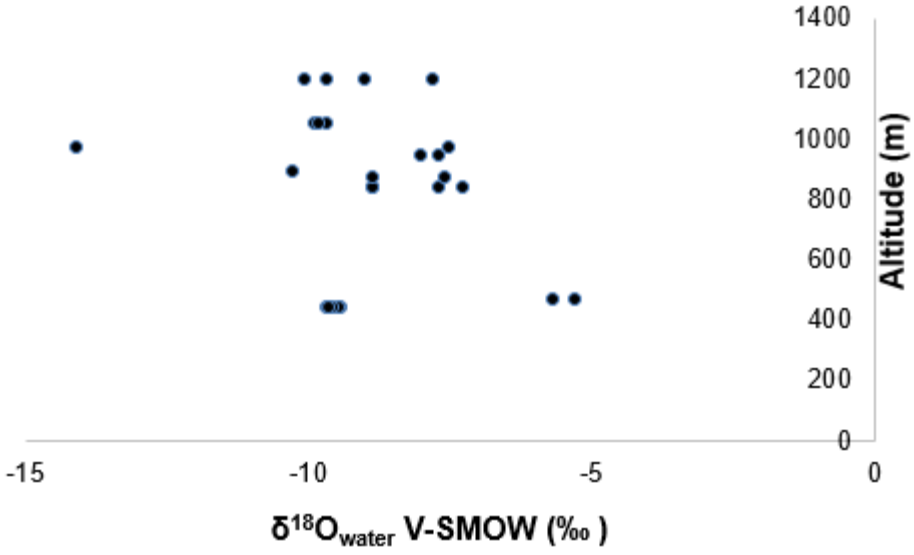
1400
1200
1000
800
600
400
200
0
Altitude (m)
-15
-10
-5
0
δ¹⁸O water V-SMOW (‰)

FIG. 6

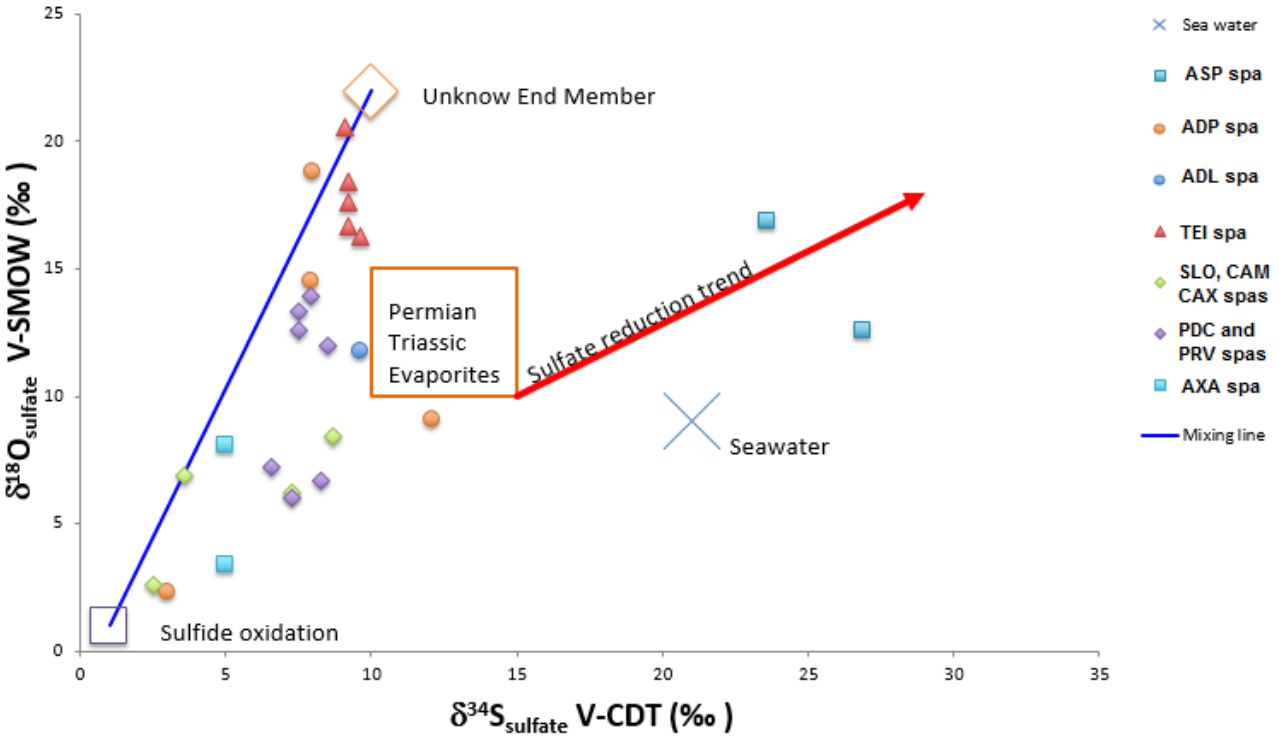
Unknow End Member
Permian
Triassic
Evaporites
Sulfate reduction trend
Seawater
Sulfide oxidation
Sea water
ASP spa
ADP spa
ADL spa
TEI spa
SLO, CAM
CAX spas
PDC and
PRV spas
AXA spa
Mixing line
δ18Osulfate V-SMOW (‰)
δ34Ssulfate V-CDT (‰)
0
5
10
15
20
25
30
35

FIG. 7

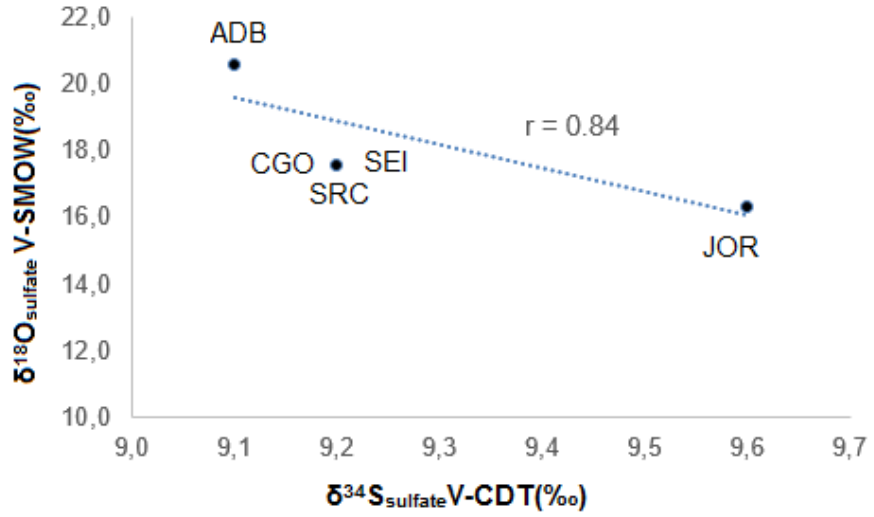
ADB
r = 0.84
CGO
SEI
SRC
JOR
22,0
20,0
18,0
16,0
14,0
12,0
10,0
9,0
9,1
9,2
9,3
9,4
9,5
9,6
9,7
δ18Osulfate V-SMOW(‰)
δ34Ssulfate V-CDT(‰)

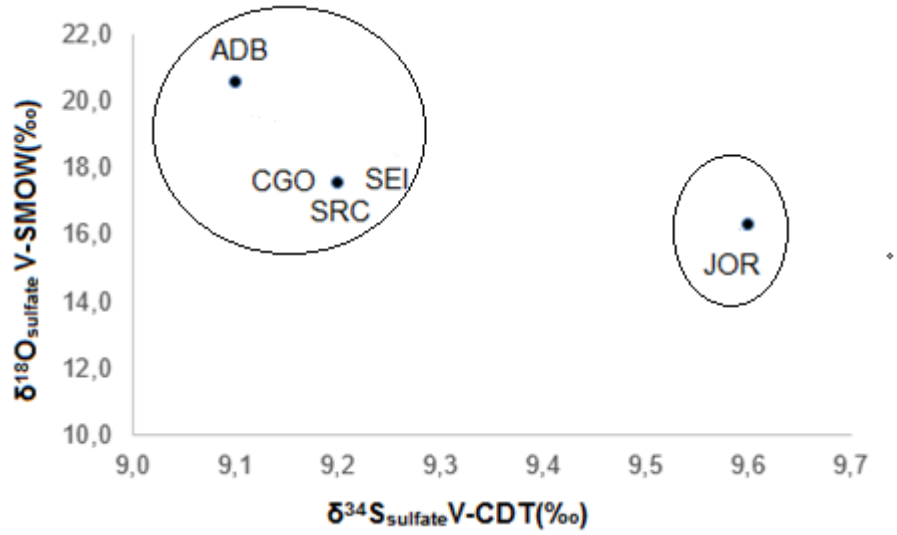
ADB
CGO
SEI
SRC
JOR
22,0
20,0
18,0
16,0
14,0
12,0
10,0
9,0
9,1
9,2
9,3
9,4
9,5
9,6
9,7
δ18Osulfate V-SMOW(‰)
δ34Ssulfate V-CDT(‰)

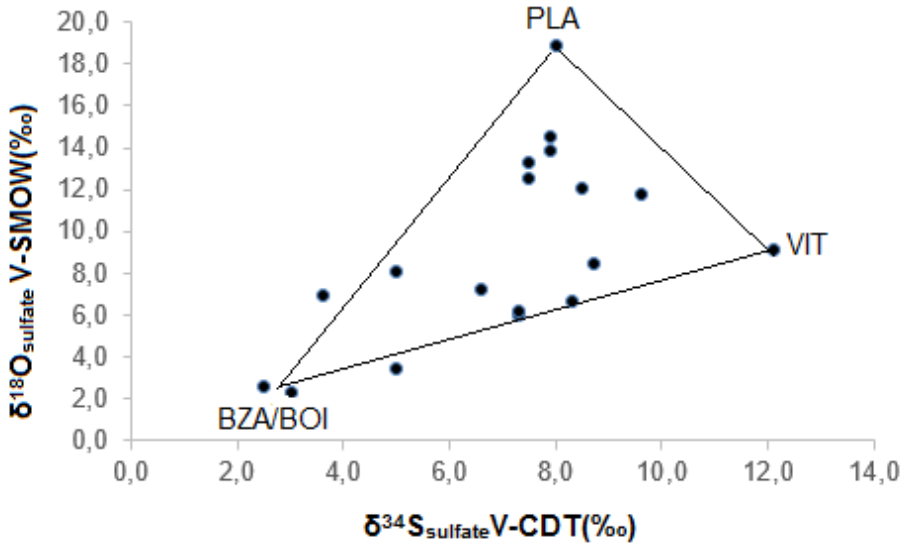
PLA
VIT
BZA/BOI
20,0
18,0
16,0
14,0
12,0
10,0
8,0
6,0
4,0
2,0
0,0
0,0
2,0
4,0
6,0
8,0
10,0
12,0
14,0
δ18Osulfate V-SMOW(‰)
δ34Ssulfate V-CDT(‰)

FIG. 8